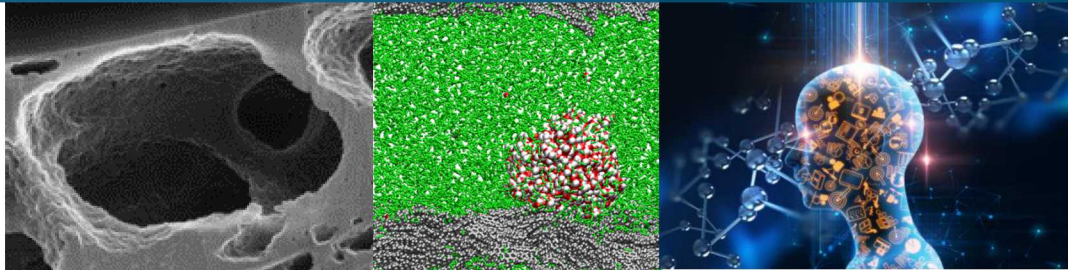




Sandia
National
Laboratories

SAND2018-12628PE

Fundamental Understanding of CH₄-CO₂-H₂O Interactions in Shale Nanopores under Reservoir Conditions



PRESENTED BY

Yifeng Wang, Tuan Anh Ho, Guangping Xu, Philippe Weck, Yongliang Xiong, Edward Matteo, Louise Criscenti, Jessica Kruichak



Sandia National Laboratories is a multimission laboratory managed and operated by National Technology & Engineering Solutions of Sandia, LLC, a wholly owned subsidiary of Honeywell International Inc., for the U.S. Department of Energy's National Nuclear Security Administration under contract DE-NA0003525.

Fundamental Understanding of CH₄-CO₂-H₂O Interactions in Shale Nanopores under Reservoir Conditions

(P.I.: Yifeng Wang, NETL POC: Bruce Brown)

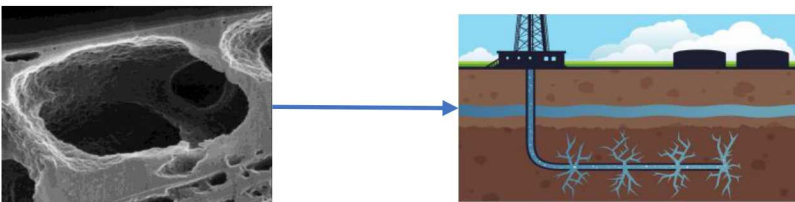


Project Goal

- Obtain a fundamental understanding of CH₄-CO₂-H₂O interactions in shale nanopores under high-pressure and high temperature reservoir conditions and integrate this understanding into reservoir engineering for efficient shale gas recovery and subsurface carbon sequestration.

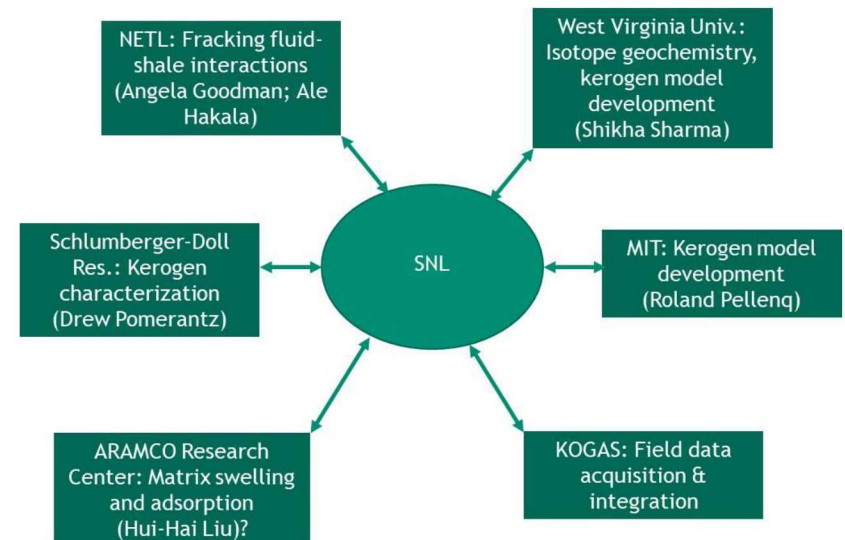
Potential Impacts

- Significantly advance fundamental understanding of hydrocarbon storage, release, and flow in shale.
- Provide more accurate predictions of gas-in-place and gas mobility in reservoirs.
- Help to develop new stimulation strategies to enable efficient resource recovery from fewer and less environmentally impactful wells.
- Provide the basic data set to test the concept of using supercritical CO₂ as an alternative fracturing fluid for simultaneous methane extraction and CO₂ sequestration.
- Leverage unique SNL capabilities: nanogeochimistry, high pressure and high temperature geochemistry, numerical modeling, and nanoscience.



Major Accomplishments and/or Deliverables (11 journal publications; 6 invited conference presentations)

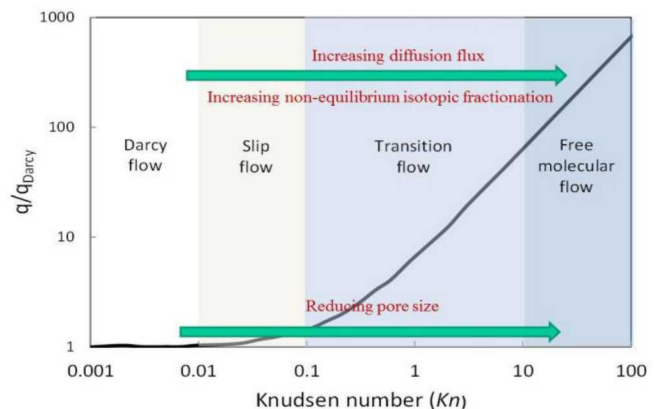
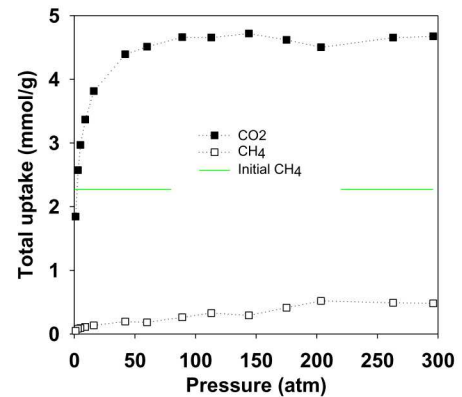
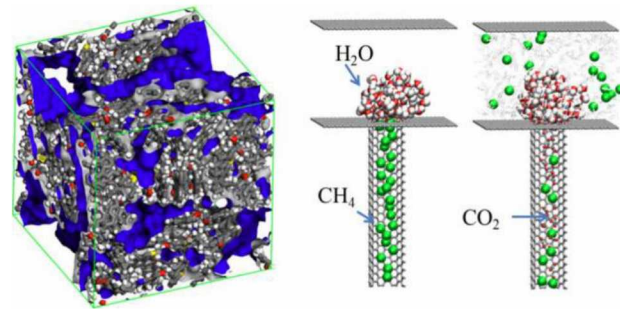
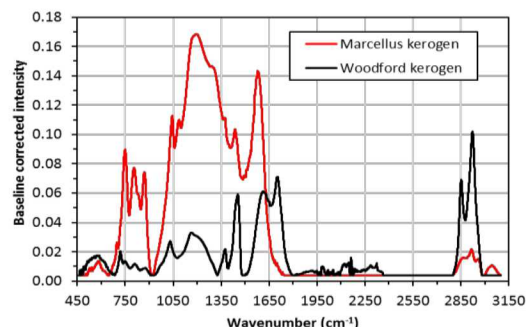
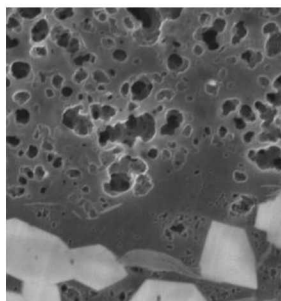
- Significant portion of CH₄ can adsorb to clay minerals.
- Wellbore production decline could be attributed to nanoscale gas disposition and migration in kerogen nanopores.
- Significant progress has been made in understanding complex interactions CH₄-CO₂-H₂O components in kerogen nanopores.
- Existing kerogen models were found inadequate in representing actual kerogen structures.
- Close collaborative relationships have been established with universities and industries.



Publications



- Xiong, Y., Wang, Y. & Olivas, T. (2015) Experimental Determination of P-V-T-X Properties and Sorption Kinetics in the $\text{CO}_2\text{-CH}_4\text{-H}_2\text{O}$ System under Shale Gas Reservoir Conditions: Part One, P-V-T-X Properties, Sorption Capacities and Kinetics of Model Materials for $\text{CO}_2\text{-CH}_4$ Mixtures to 125°C, **High Temperature Aqueous Chemistry**, HiTAC-II Workshop, Heidelberg, April 16, 2015.
- Ho, T. A., Criscenti, L. J. & Wang, Y. (2016) Nanostructural control of methane release in kerogen and its implications to wellbore production decline. **Scientific Reports** 6, 28053; doi: 10.1038/srep28053.
- Weck, P. F., Kim, E. & Wang, Y. (2016) van der Waals forces and confinement in carbon nanopores: Interaction between CH_4 , COOH , NH_3 , OH , SH and single-walled carbon nanotubes. **Chem. Phys. Lett.** 62, 22-26.
- Cristancho, D., Akkutlu, I.Y., Criscenti, L.J., Wang, Y. (2016) Gas storage in model kerogen pores with surface heterogeneities, **SPE-180142-MS**, DOI: 10.2118/180142-MS.
- Wang, Y. (2017) On subsurface fracture opening and closure. **J. Petrol. Eng.** 155, 46-53.
- Wang, Y. (2018) From nanofluidics to basin-scale flow in shale: Tracer investigations, In: **Shale Subsurface Science and Engineering** (in press, book chapter)
- Weck, P. F. Kim, E., Wang, Y. et al. (2017) Model representation of kerogen structures: An insight from the density functional theory. **Scientific Reports**, 7, DOI:10.1038/s41598-017-07310-9.
- Ho, T. A., Greathouse, J. A., Wang, Y. and Criscenti, L. J. (2017) Atomistic structure of mineral nano-aggregates from simulated compaction and dewatering. **Scientific Reports**, 7, 15286.
- Ho, T. A., Wang, Y., Criscenti, L. J. & Xiong, Y. (2017) Differential retention and release of CO_2 and CH_4 in kerogen nanopores: Implications to gas extraction and carbon sequestration. **Fuel**, 220, 1-7.
- Ho, T. A. Wang, Y. and Criscenti, L. J. (2018) Chemo-mechanical coupling in kerogen gas adsorption/desorption. **Phys. Chem. Chem. Phys.**, 20, 1239.
- Ho, T. A. Wang, Y. et al. (2018) Supercritical CO_2 -induced atomistic lubrication for water in a rough hydrophilic nanochannel. **Nanoscale** (online now)
- Wang, Y. et al. (2019) Nanogeochemistry of unconventional oil/gas reservoirs (invited paper by **Chemical Geology**).
- Book: Wang, Y., **Nanogeochemistry: Emergent Properties of Nano-Scale Mineral Phases and Confined Fluids**, Elsevier (in preparation).



Why do we care?



Sustainability of shale oil/gas production:

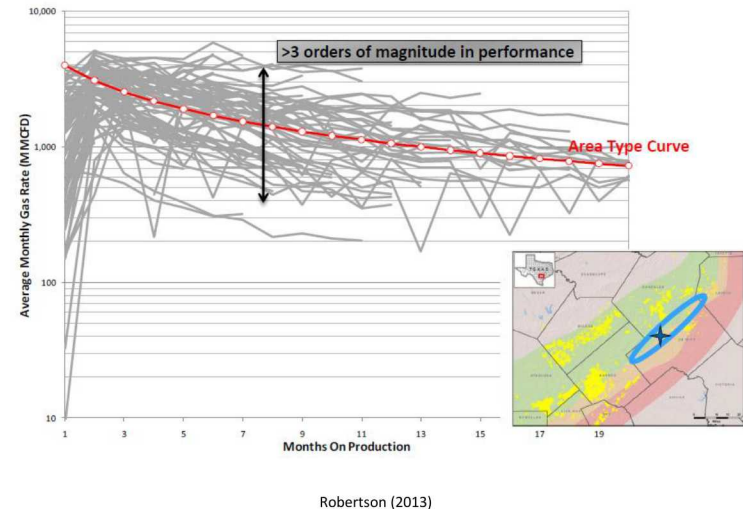
- Large variability and unexpected rapid decline in well production (up 95% reduction over first 3 years)
- New wells to be drilled to maintain the supply, with increasing cost/well
- Low recovery rates (<10%), with little known about secondary gas recovery in “brown fields” (>90% of total gas reserve!!!).
- Long-term production projection largely empirical

Locating sweet spots, maximizing individual wellbore production while minimizing environmental impacts.

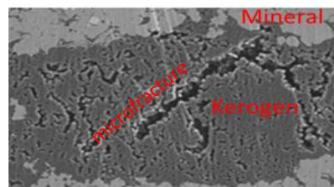
- Existing practice largely empirical.

Limiting step of oil/gas production:

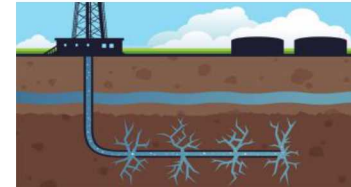
- Fluid interaction and transport in nanoporous shale matrix
- Knowledge drawn from conventional reservoirs is not applicable.
- Mechanistic understanding of oil/gas disposition and release in shale matrix is crucial for developing engineering approach to maximizing wellbore production and extending the production cycle.



Oil/gas release from kerogen pores (Pore size: nanometer scale)



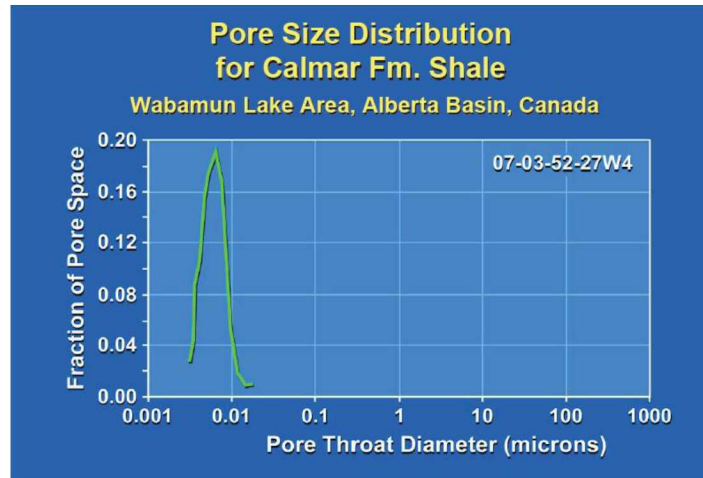
Fluids “flow” from kerogen via nano- or micro-fractures (Channel size: nanometer to micrometer scale)



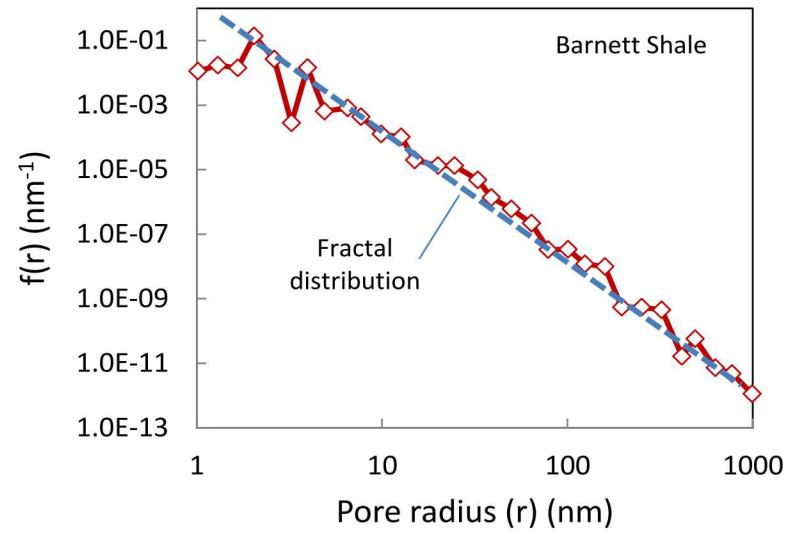
Fluids flow into hydraulic fractures then to production well (Channel size: millimeters to decimeters)

Limiting step(s)

Why nanoscale?

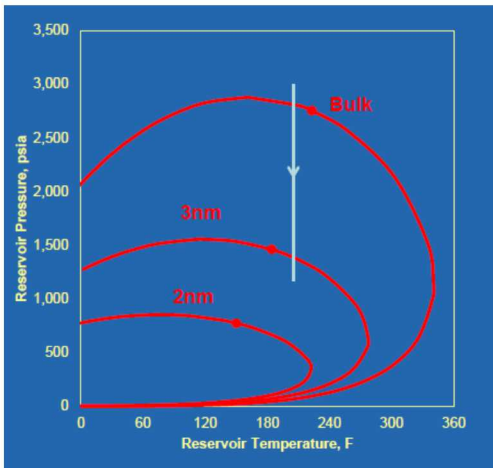


Bachu & Bennion (2006)

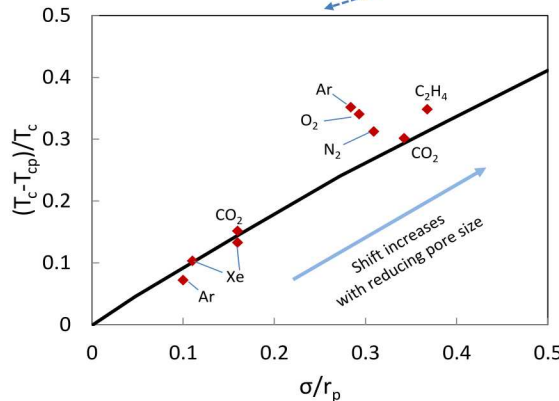


Clarkson et al. (2012)

Effects of nanopore confinement



Akkutlu, 2013



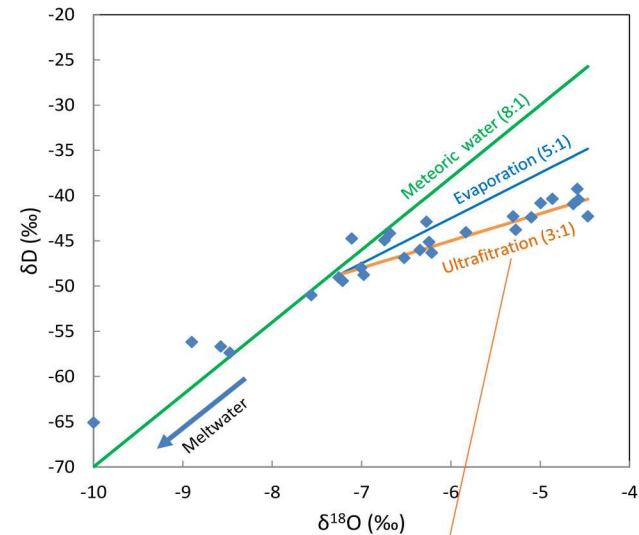
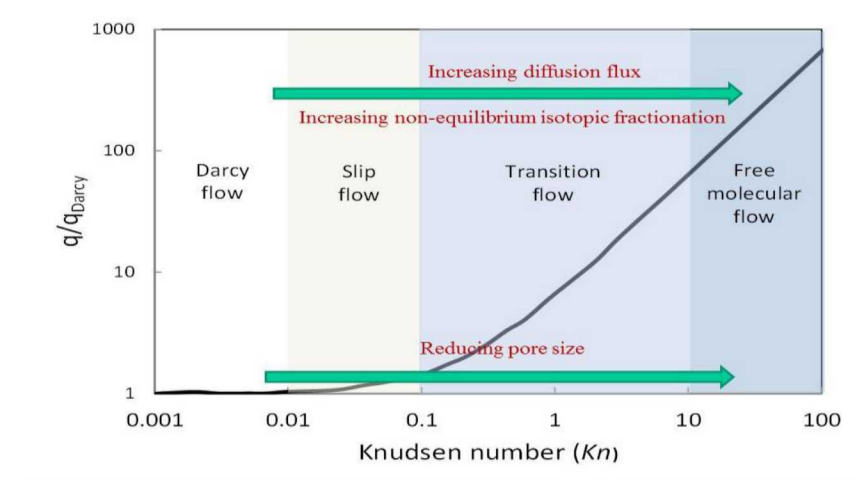
Wang (2014); Zarragoicoechea and Kuz (2004)

Rule of thumb: Chemical species under nanoconfinement behave drastically differently from those unconfined (i.e., those in bulk phase). Nanoconfinement modifies:

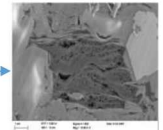
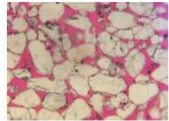
- Thermodynamic properties
- Kinetic properties
- Transport properties
- Others

Most of the knowledge obtained from conventional reservoirs is not applicable to shale oil/gas.

Emergent transport properties in nanopores: Isotopic fractionation as unique signature for real time monitoring for gas production



Conventional reservoir



Shale formation

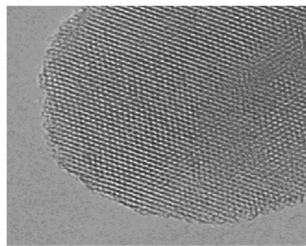
$$k_{app} = \frac{2r}{3RT} \left(\frac{8RT}{\pi M} \right)^{1/2} + \left[1 + \left(\frac{8\pi RT}{M} \right)^{1/2} \frac{\mu}{pr} \left(\frac{2}{\alpha} - 1 \right) \right] \frac{cr^2}{8\mu}$$

Wang (2018)

M - Molecular weight

Mass dependent transport

Technical Approach



Synthesis of nanoporous materials



Isolation of kerogen from Mancos shale



Nanoge geochemistry: Nanostructures, emergent properties and their control on geochemical reactions and mass transfers

Yifeng Wang

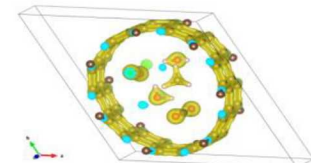
Sandia National Laboratories, P.O. Box 5800, Albuquerque, NM 87185-0776, USA

ARTICLE INFO

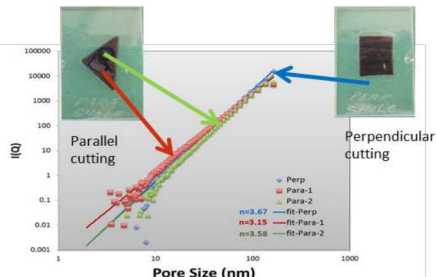
Article history:
Received 14 November 2013

ABSTRACT

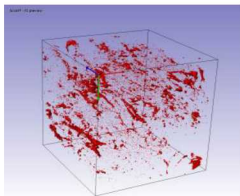
Nanoge geochemistry—a newly emerging research field—attempts to understand geochemical reactions in a new dimension to elucidate where molecular-scale control on the chemical reactions



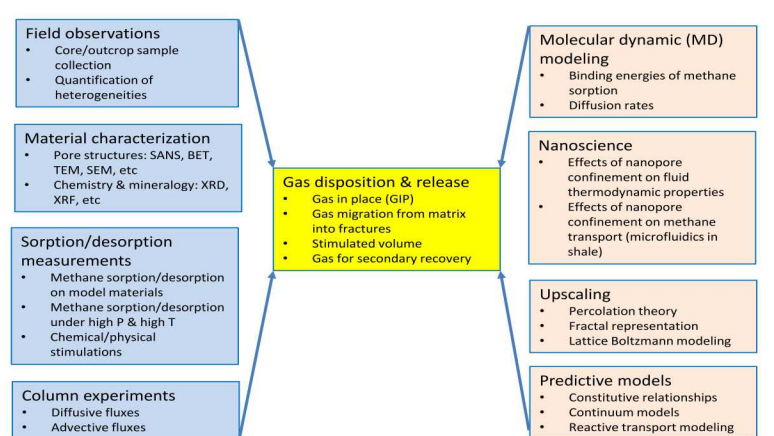
Density functional theory (DFT) modeling



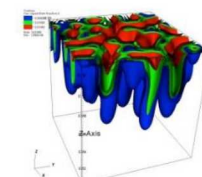
Pore structure characterization



Pore structure characterization (FIB)

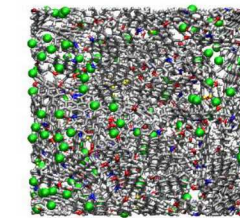


High pressure/high temperature sorption/desorption measurements

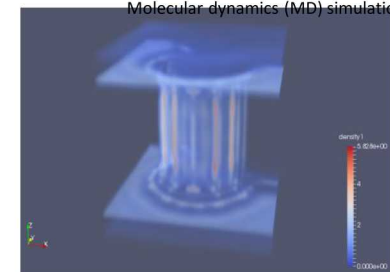


<http://www.pfotran.org/applications.html>

PFLOTRAN: Reactive transport modeling

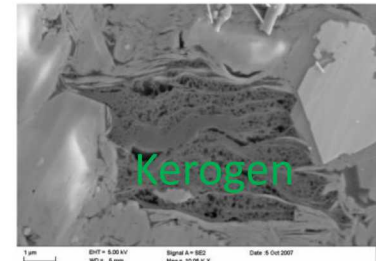


Molecular dynamics (MD) simulation



TRAMANTO: Classical Density Functional Theory

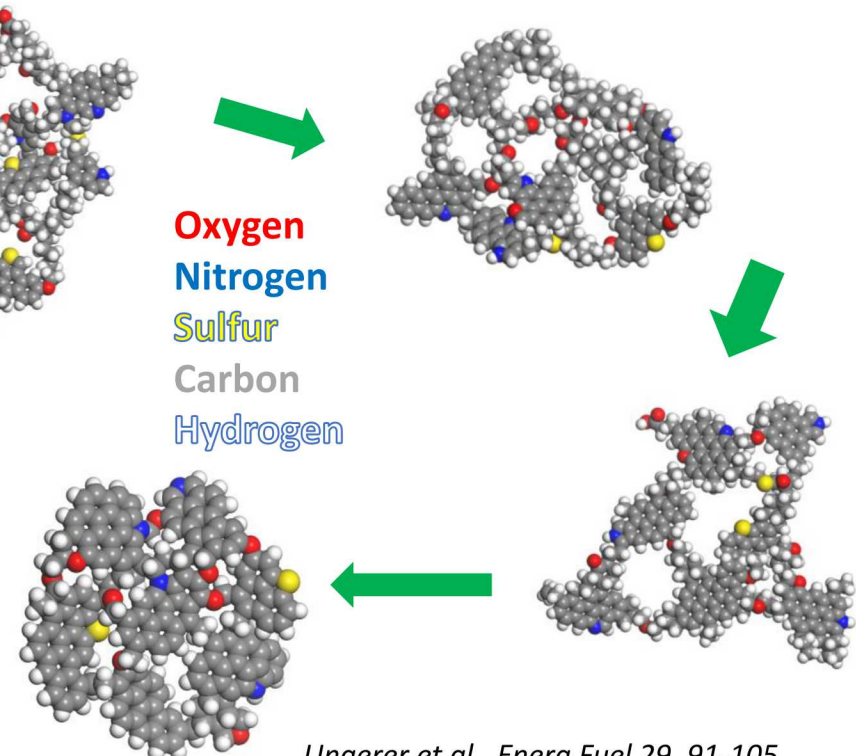
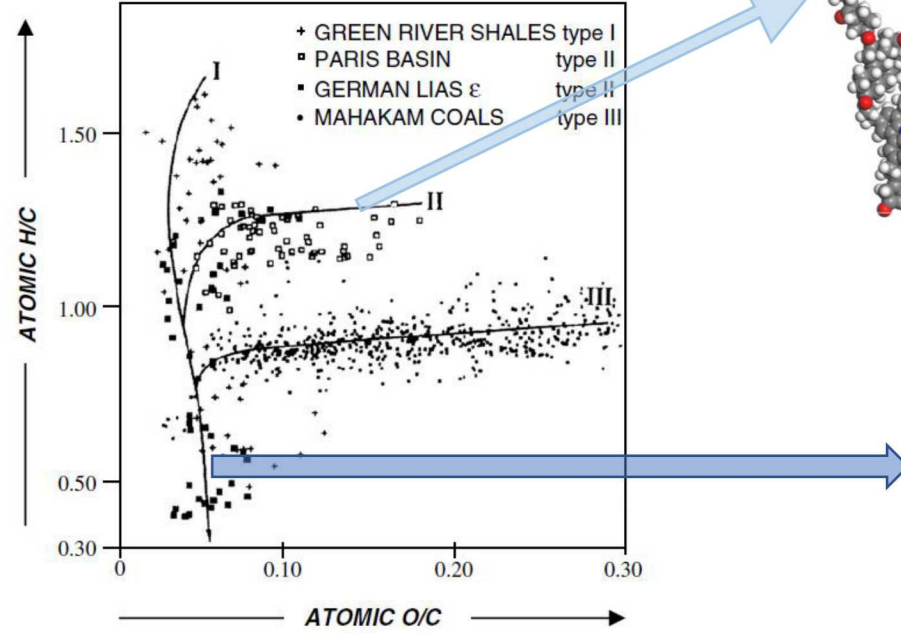
Kerogen 101



- Insoluble organic matter found in sedimentary rocks (geochemistry)
- Cracks into petroleum products (kerogen maturation, petroleum generation)

Van Krevelen diagram

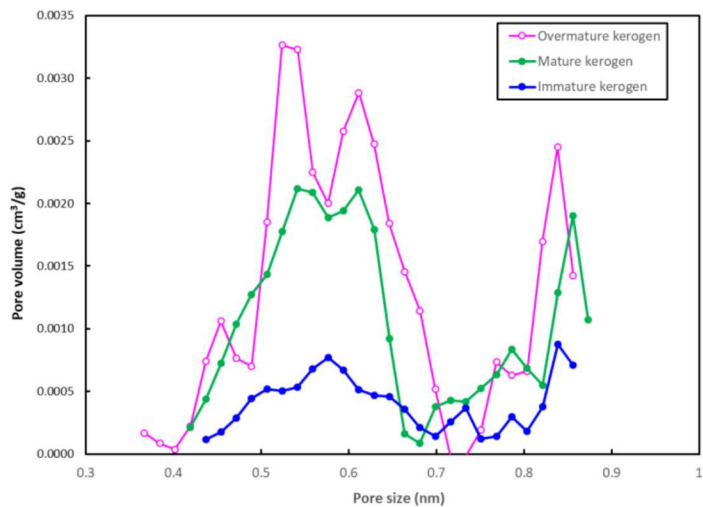
Organic Geochemistry 38, 719-833 (2007)



Ungerer et al., Energ Fuel 29, 91-105

- Hosts pore space responsible for petroleum storage and transport

Kerogen characterization



BET measurements

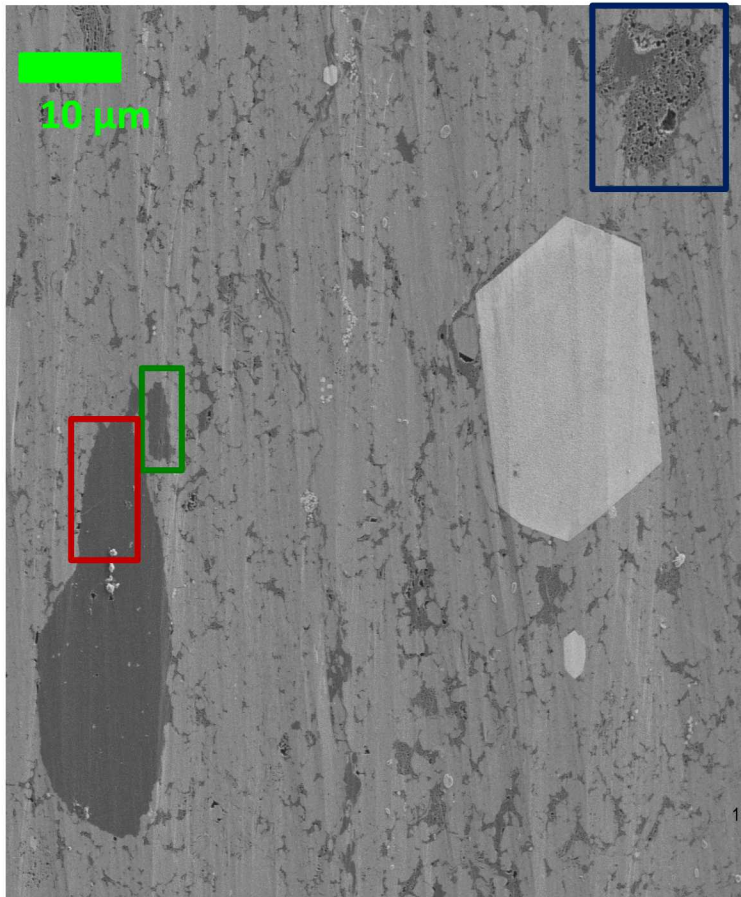
	Ro%	BET (m ² /g)	Pore volume (< 0.9 nm) cm ³ /g	Micropore volume (< 2 nm) cm ³ /g	Mesopore volume (2-50 nm) cm ³ /g
Immature	0.7	54	0.011	0.020	0.150
Mature	1.4	205	0.029	0.080	0.393
Overmature	2.5	301.5	0.038	0.131	0.395
CO ₂ swelled overmature		281.7	0.035	0.105	0.348

NMR ¹³C analyses of kerogen

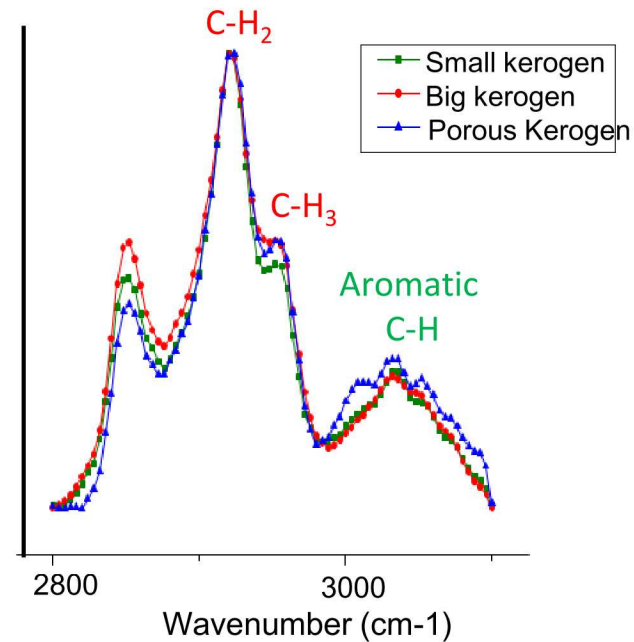
	Aromatic			Aliphatic		
	alkene ring and benzyl ring			-CH ₂ -	alkane (-CH ₃)	
	124 ppm	110 ppm	total		30 ppm	19 ppm
Mature kerogen	89.81%	4.81%	94.6%	2.03%	3.35%	5.4%
Overmature kerogen	86.27%	11.18%	97.5%	0.36%	2.19%	2.6%
Activated carbon	66.27%	33.73%	100%			

Compositional and structural heterogeneity of kerogen

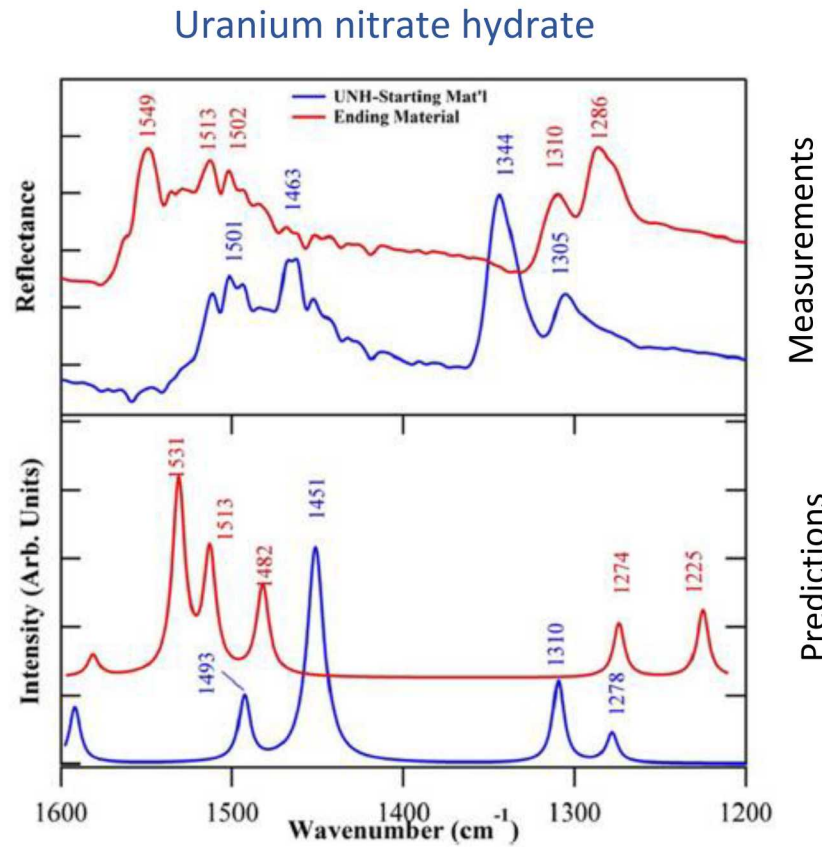
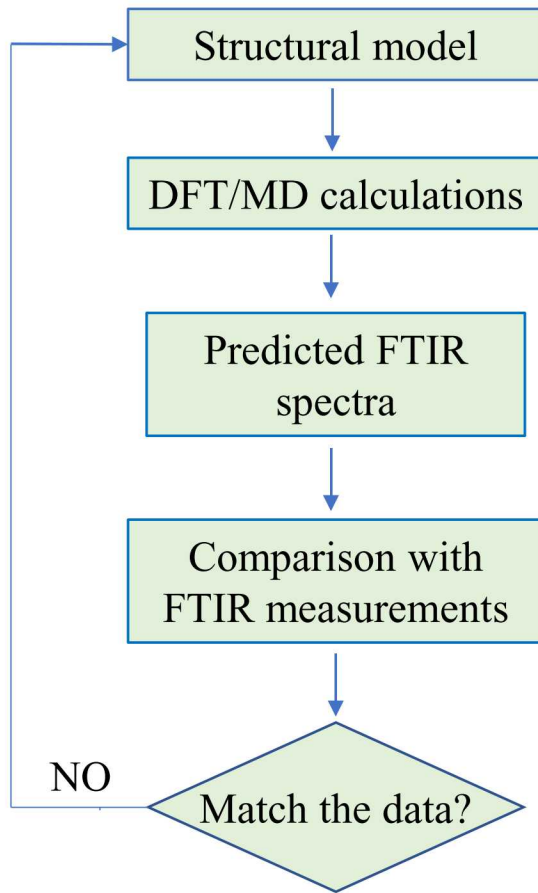
NanolR spectra of different kerogen grains



- Strong aromatic absorption – mature kerogen
- Subtle differences in composition between porous and non-porous kerogen grains

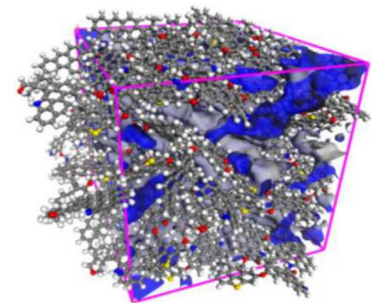
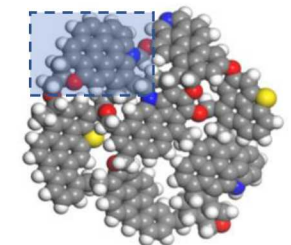
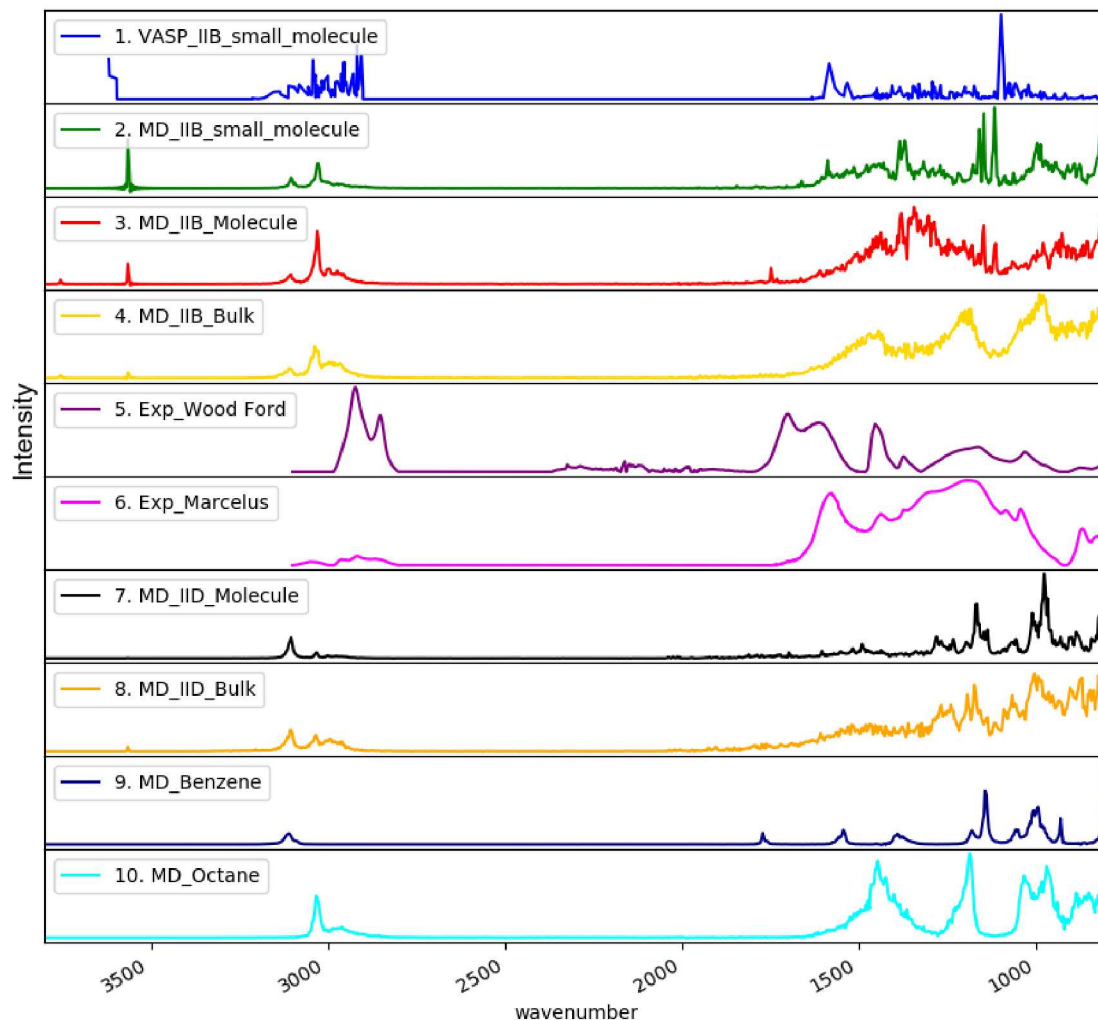


Testing adequacy of existing kerogen structural models: Approach



Johnson et al. (2015)

Adequacy of existing kerogen structural models



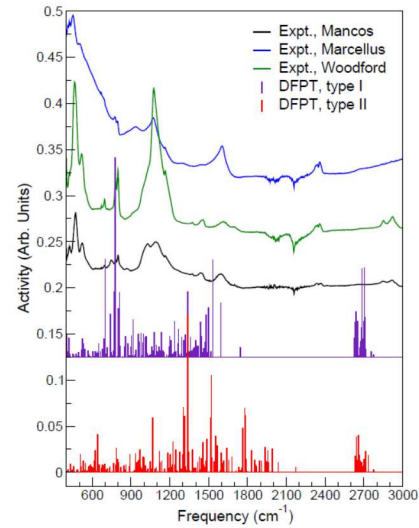
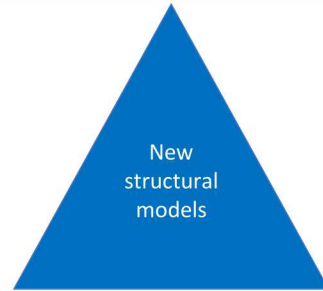
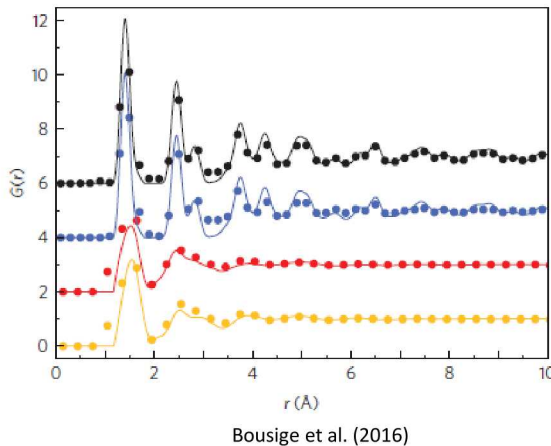
- A significant gap exists in the representation of functional groups.
- Existing force field for MD simulations needs to be refined.

Development of new kerogen models

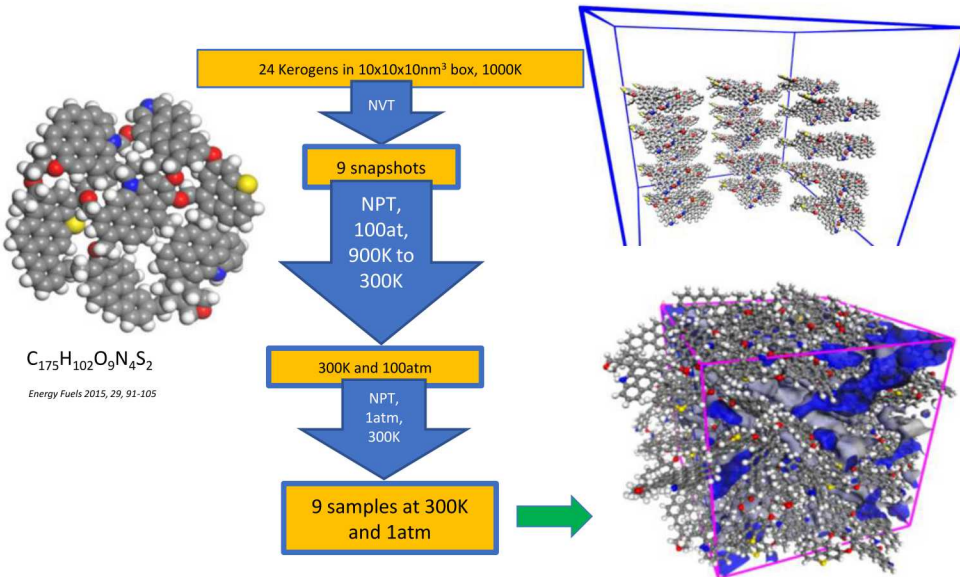
Table 1
Composition and structural parameters of the type II kerogen.^a

Property	Quantity	Immature		Oil window		Postmature	
		Analytical data	Model unit	Analytical data	Model unit	Analytical data	Model unit
Composition	H/C	1.17	1.17	0.89	0.905	0.56	0.58
	O/C	0.097	0.095	0.05	0.054	0.047	0.051
	N/C	0.029	0.024	0.021	0.021	0.021	0.023
	S/C	0.014	0.012	0.006	0.008	0.01	0.011
C group	Aromatic C from XPS(a) or NMR(b) (%)	40(a), 40(b)	41	54(a), 54(b)	58.7	72(a), 80(b)	79
	C atoms per aromatic cluster	12	11.4	19	20.3	20	19.9
	Fraction of attached aromatic C	0.43	0.46	0.30	0.28	0.24	0.28
	Protonated aromatic C (per 100 C)	13	14	17	14	28	25
O group	O in C—O per 100 C	5.0(a), 7 (b)	5.2	3.5(a), 5 (b)	3.7	4.7(a), 2 (b)	5.1
	O in carboxylic groups (—COOH) per 100 C	1.3	1.6	0.7	0.83	0	0
	O in carbonyl groups (>C=O) per 100 C	3.4	2.8	0.8	0.83	0	0
N groups	Pyrrolic (mol% of N)	52	66	65	60	62	75
	Pyridinic (mol% of N)	27	17	18	40	15	25
	Quaternary (mol% of N)	18	17	17	0	23	0
S Groups	Aromatic S (mol% of S)	46	67	54	50	80	100
	Aliphatic S (mol% of S)	54	33	46	50	20	0

^a The analytical data corresponds to the experimental work of Kelemen et al. [24]. The model data corresponds to the molecular models of kerogen (type IIA, IIC and IID) detailed in the paper by Ungerer et al. [41].



Construction of condensed kerogen structures



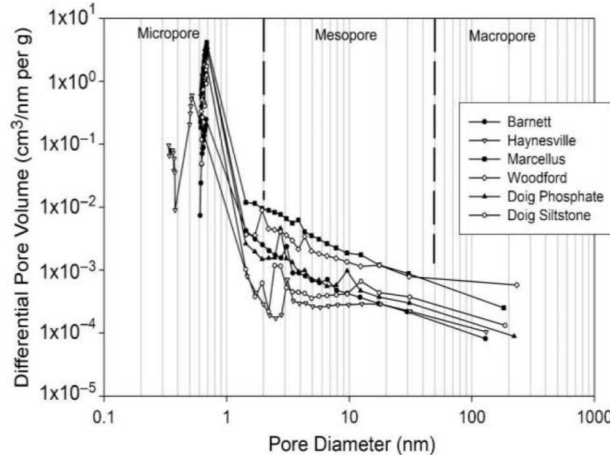
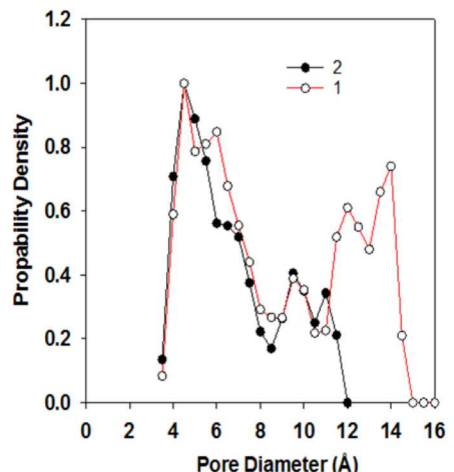
Density

Average : $1.22 \pm 0.04 \text{ g/cm}^3$

Experiment: $1.28 \pm 0.3 \text{ g/cm}^3$

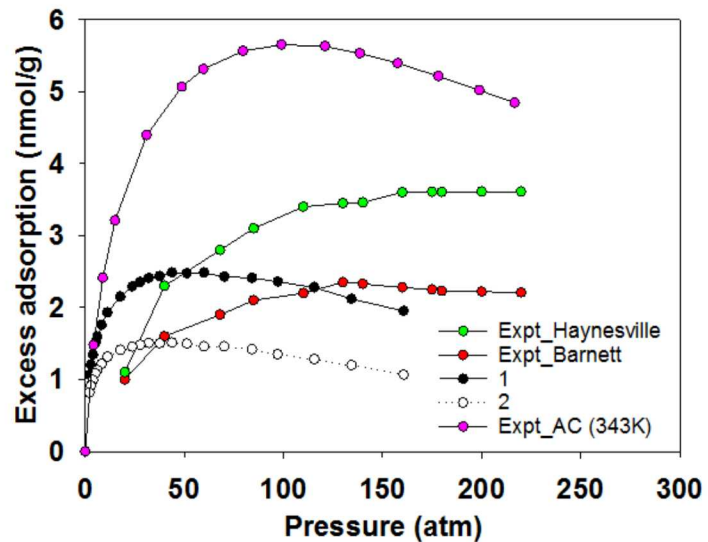
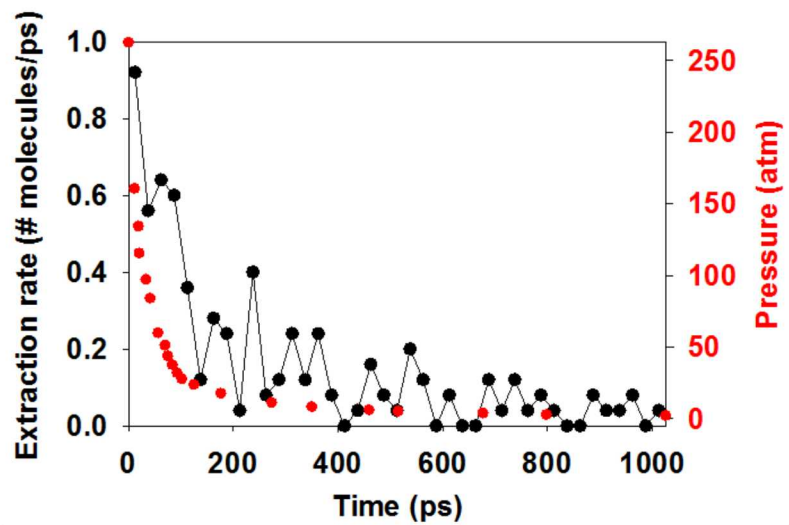
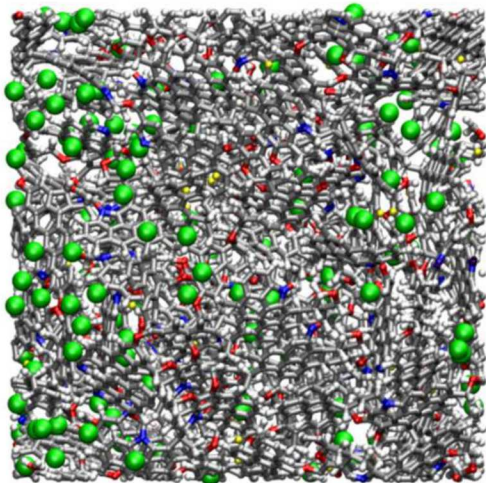
Stankiewicz A, et al. (2015) Kerogen density revisited – lessons from the Duvernay Shale. In: Paper URTeC 2157904 at the Unconventional Resources Technology Conference, San Antonio, Texas, July 2015

Pore size distribution



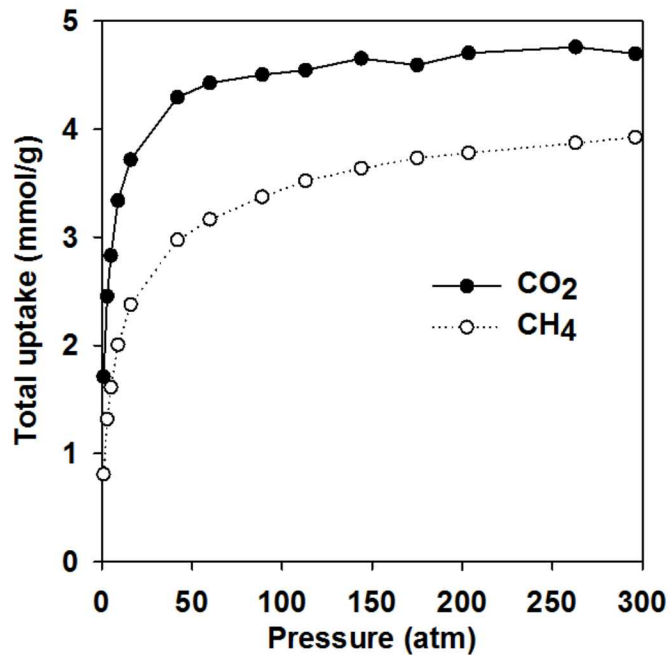
AAPG 96 (2012), 1099-1119

Methane sorption and release within kerogen

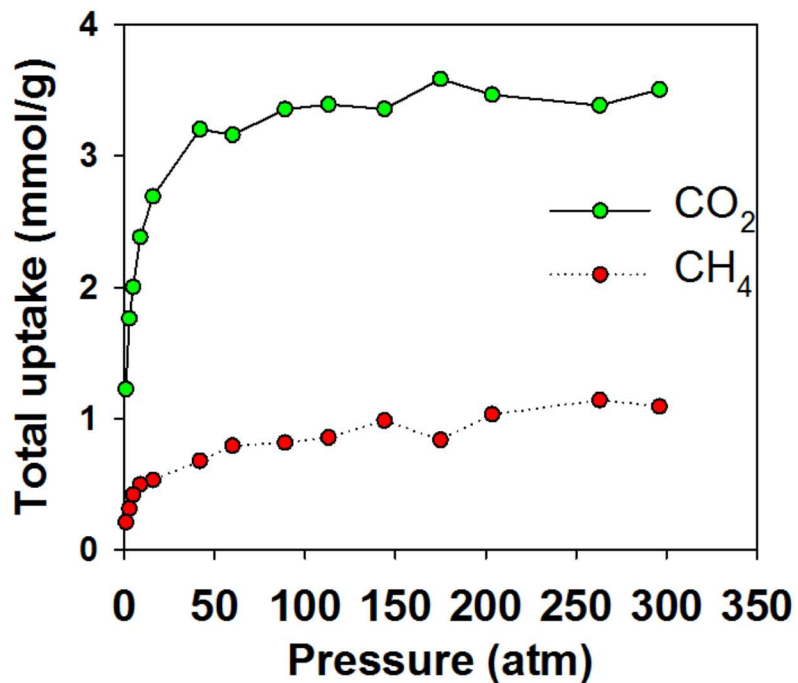


Differential retention and release of CO_2 and CH_4 in kerogen nanopores (Fuel 220, 1-7, 2018)

Pure gas adsorption



1:1 binary gas adsorption



Kerogen preferentially retains CO_2 over CH_4 .

Simultaneous shale gas extraction and carbon sequestration.

Kerogen swelling: Chemo-mechanical coupling (PCCP, 2018)

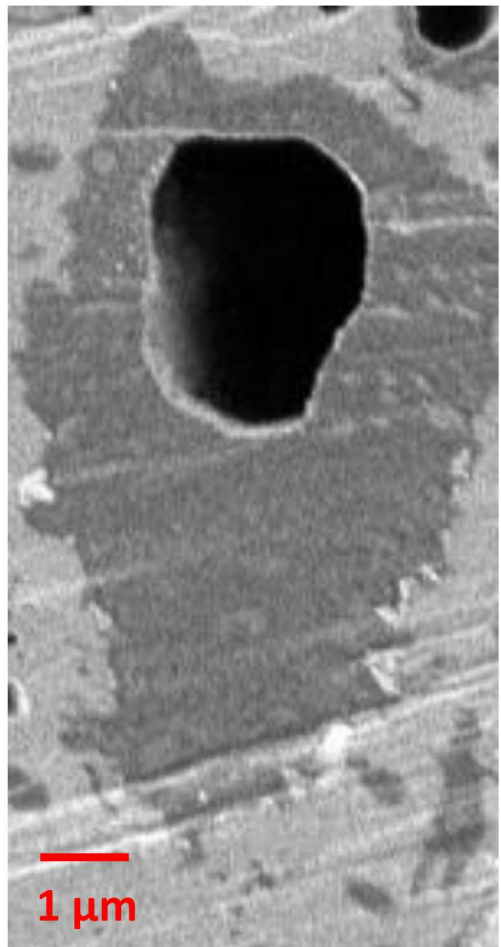
Rubber swelling in oil



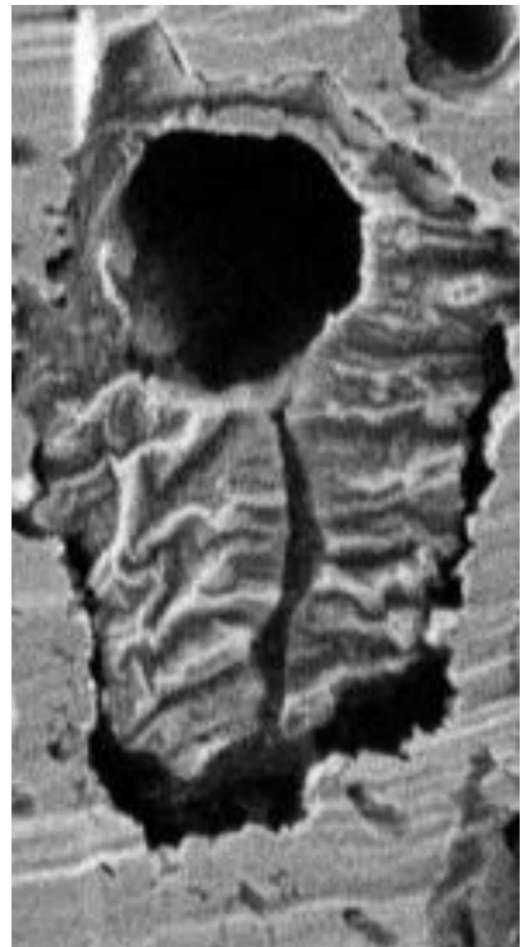
From: Drew Pomerantz,
Schlumberger



Will kerogen swell upon
gas adsorption?



Intact shale with swelled
kerogen

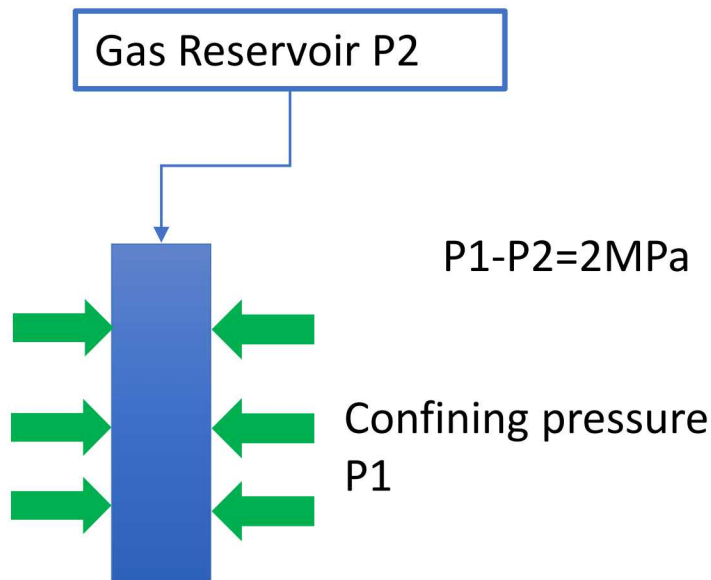


Bitumen-extracted shale with
collapsed kerogen

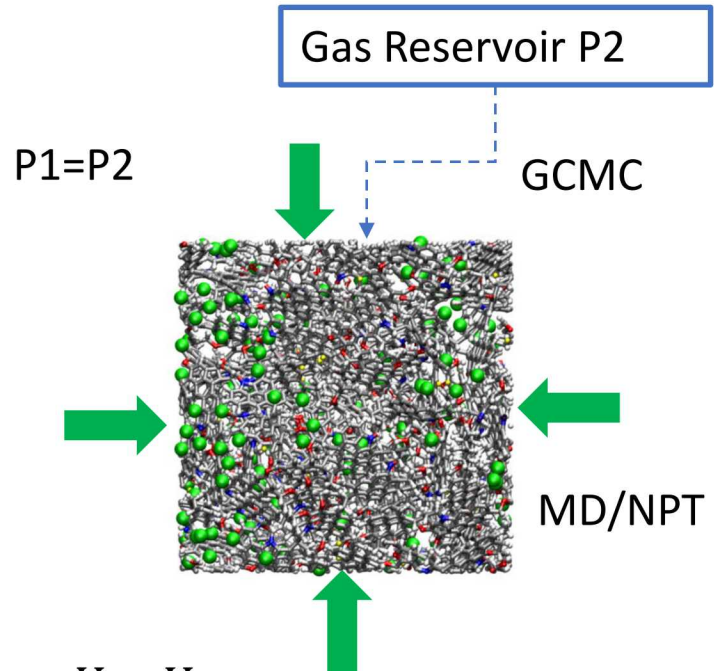
Kerogen swelling: Model setup

Experimental setup

(J. Unconv. Oil Gas Resour., 2014)



Simulation: Hybrid MD/MC

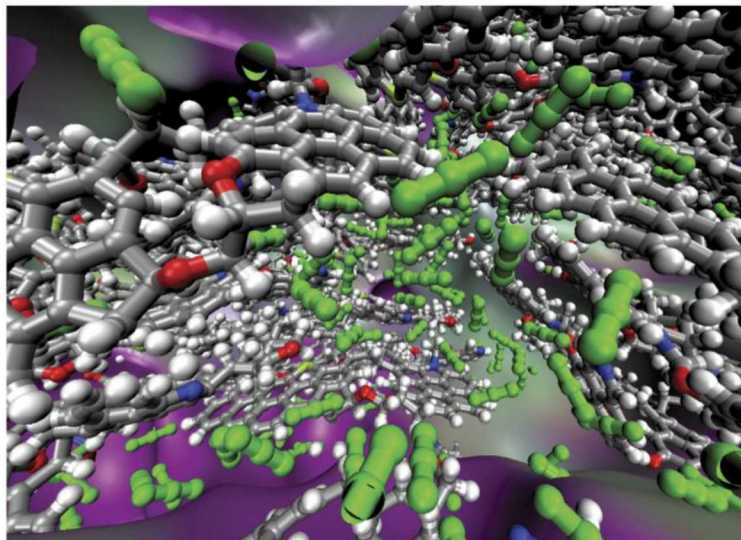
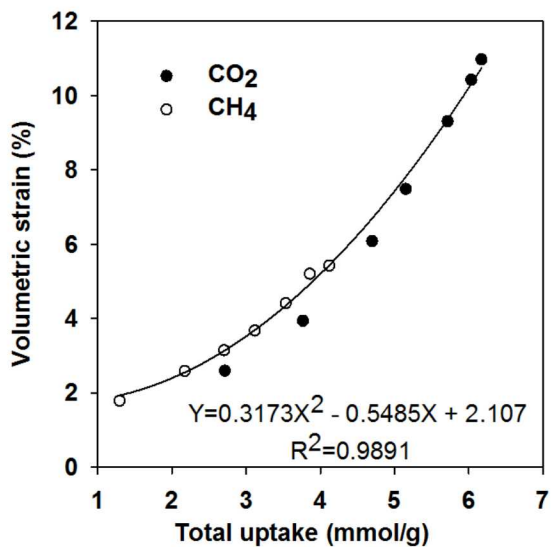
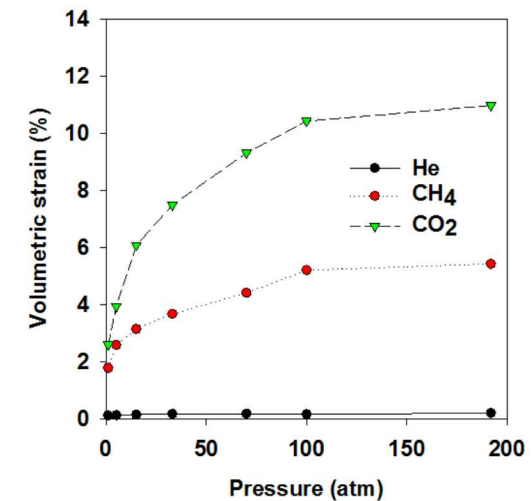


$$\text{Volumetric strain} = \frac{V - V_o}{V_o}$$

V : kerogen volume after gas adsorption

V_o : kerogen volume before gas adsorption

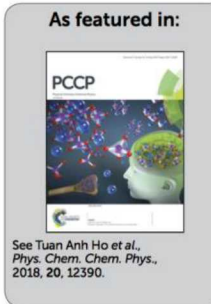
Kerogen swelling: Simulation results



Highlighting shale gas research from the Geoscience Group, Sandia National Laboratories, NM, USA. This work was conducted by Dr Tuan Ho, thanks to funding granted to Dr Yifeng Wang by the DOE National Energy Technology Laboratory.

Chemo-mechanical coupling in kerogen gas adsorption/desorption

We use an integrated experimental and modeling approach to fundamentally understand the interaction of gas and fluid with kerogen and clay under reservoir conditions. Specifically, nanostructural properties of subsurface porous media, gas adsorption and release from the kerogen network, deformation of shale associated with adsorption and lithostatic stress, and wettability of inorganic and organic matter.

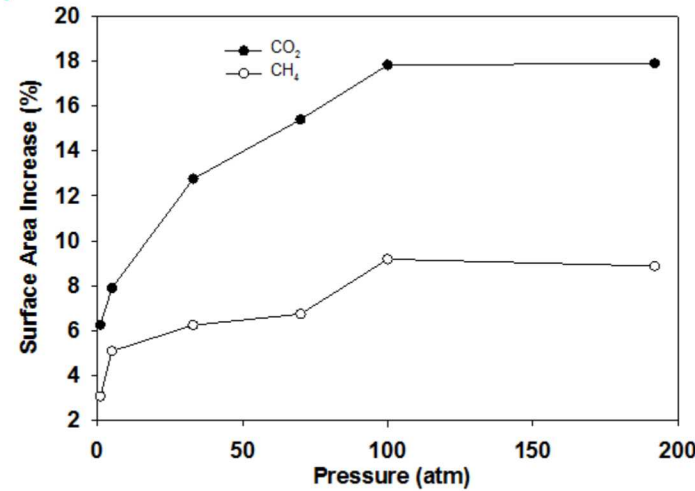
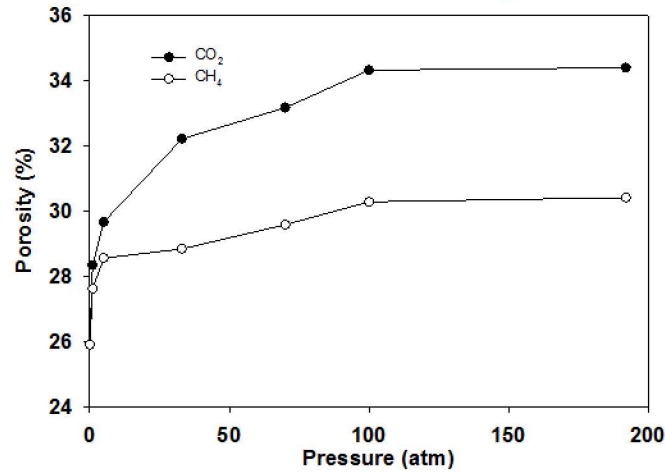


rsc.li/pccp
Registered charity number: 207890

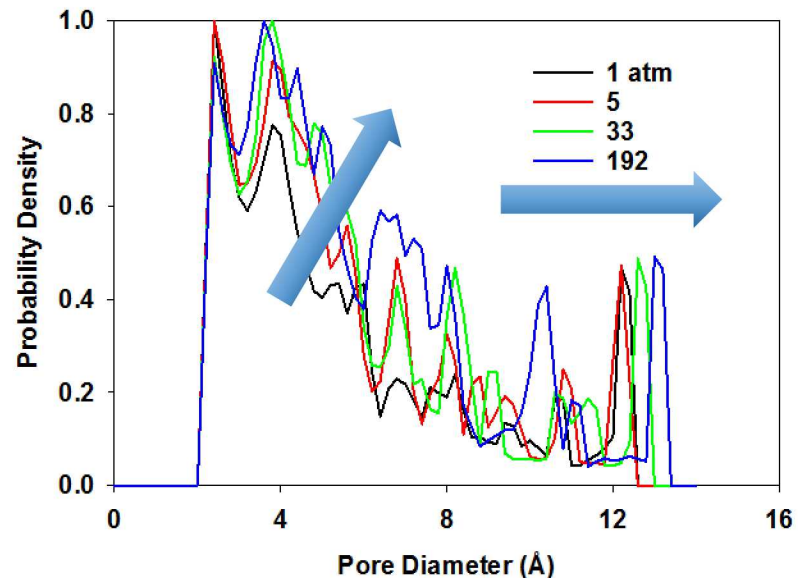
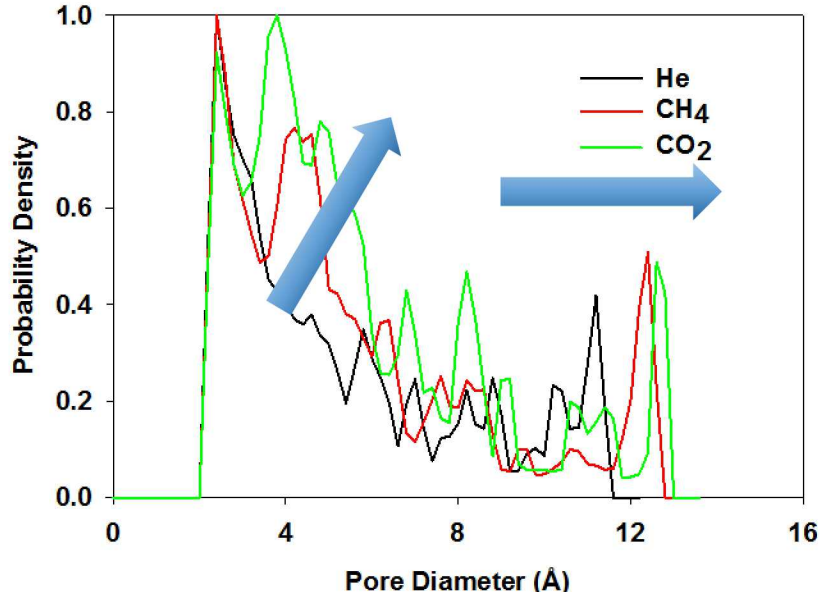
Swelling seems controlled by the surface layer of gas adsorbed.

Kerogen swelling: Effects of gas type and pressure

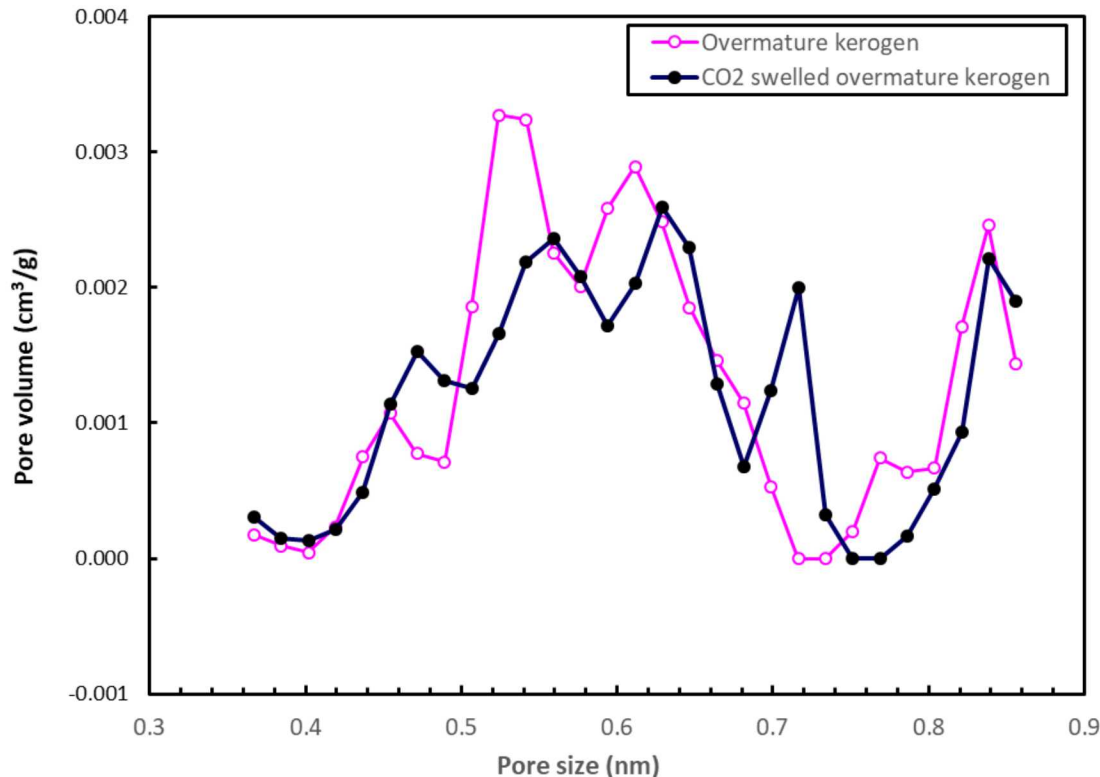
Effects of kerogen swelling on porosity and surface area



Effects of kerogen swelling on pore size distribution



Kerogen swelling: Experimental observations

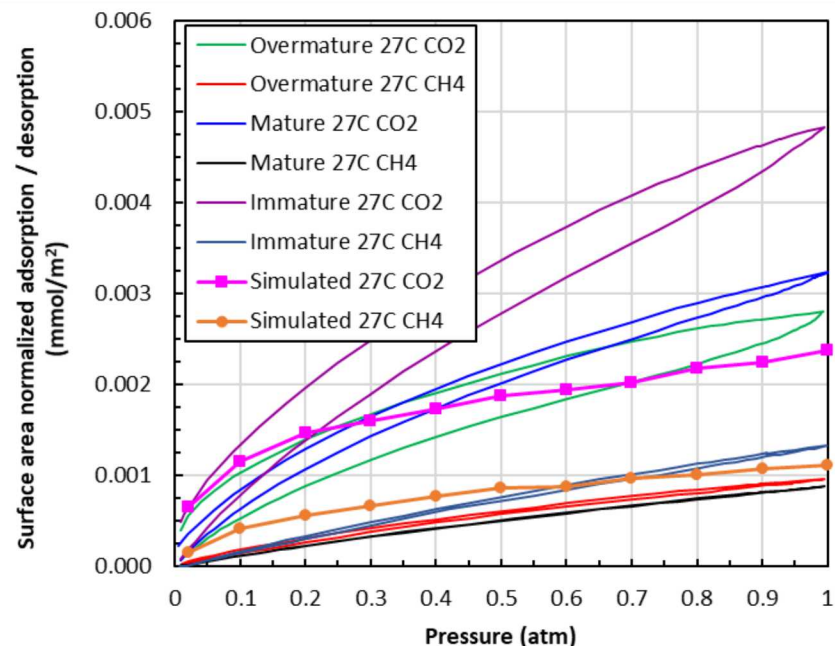
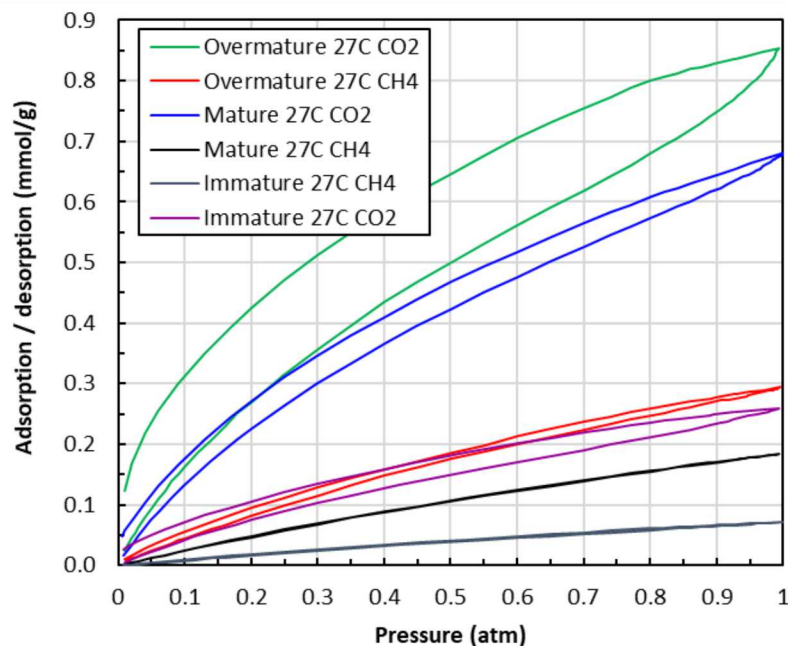


Kerogen is filled with 1 atm CO_2 and sealed for 4 months before being remeasured

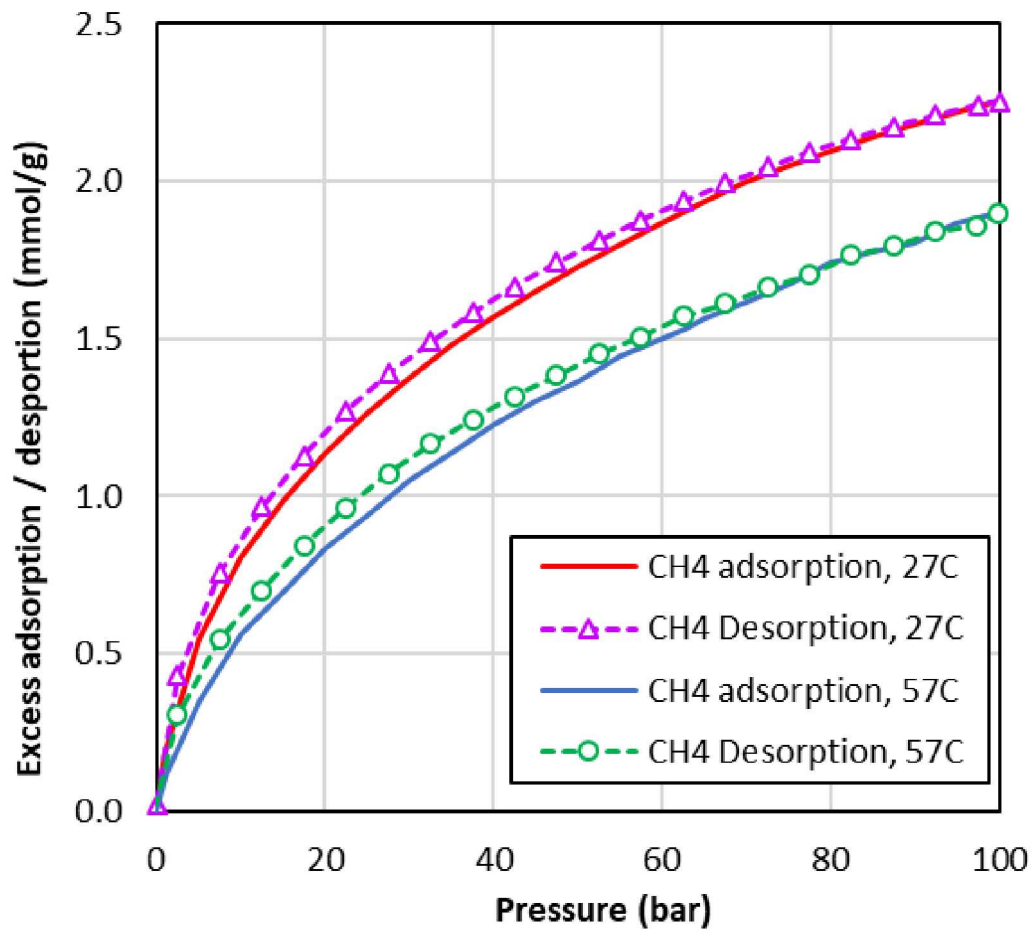
- Kerogen is mechanically compliant?!
- Implications to reservoir engineering, especially, for organic carbon-rich plays.

Gas adsorption and desorption on kerogen: Hysteresis loop

- From immature to mature to overmature, adsorption ability increases with maturity; however, after the normalization of surface area, the trend is reversed, suggesting a possible control by functional groups.
- The simulated CO_2 and CH_4 adsorption curves for overmature kerogen are in agreement with the measured values.

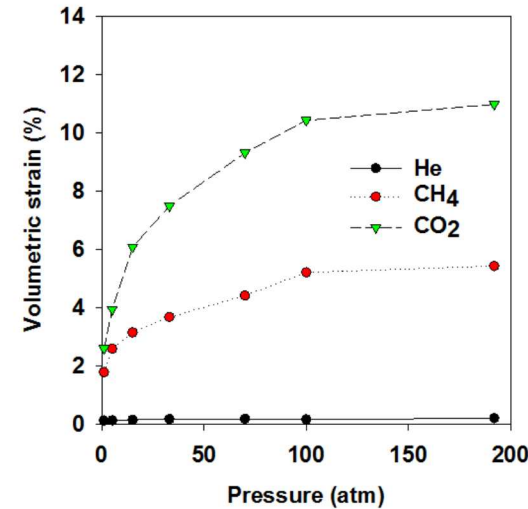
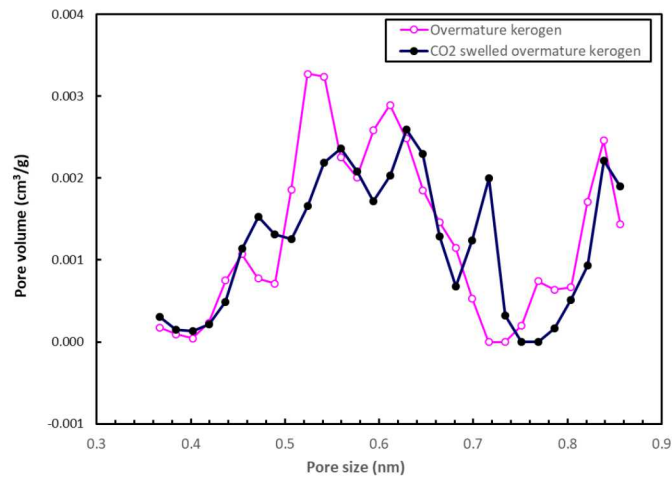
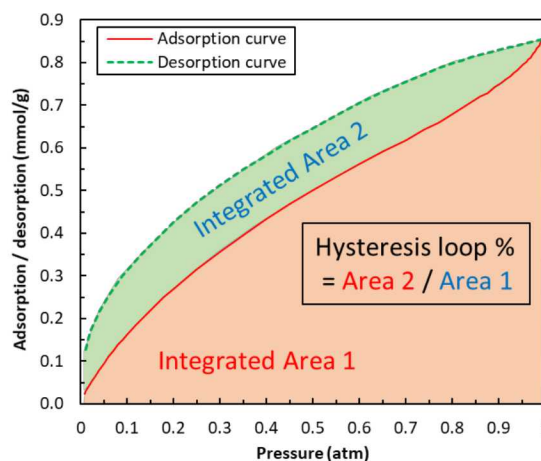


Gas adsorption and desorption on kerogen: High pressure measurements



Hysteresis loop exists for very high pressure adsorption.

Understanding adsorption-desorption hysteresis



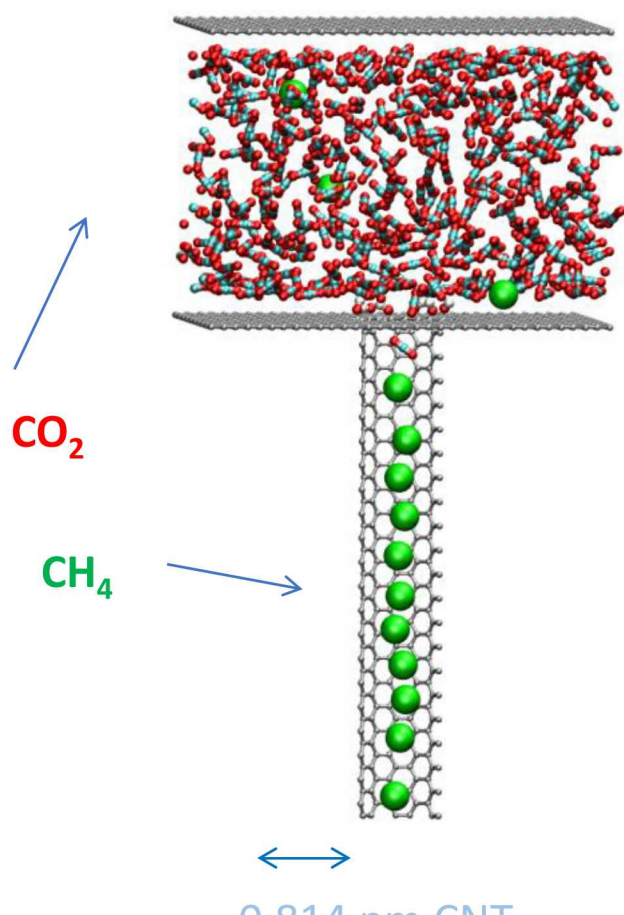
Hysteresis loop %		BET surface area (m²/g)	Pressure from 0 to 1 atmosphere					Pressure: 0 to 100 bar	
			N ₂ 77K	27 °C CO ₂	57 °C CO ₂	27 °C CH ₄	57 °C CH ₄	27 °C CH ₄	57 °C CH ₄
Marcellus	immature	54	21.3%	18.6%		4.8%			
	mature	205	38.1%	9.5%		0.9%			
	overmature	301.5	14.0%	27.1%	44.8%	6.2%	11.8%	2.8%	3.5% / 5.6%*
Woodford	immature	50	12.6%	16.2%	23.0%	2.9%	4.3%		
Carbon Black		31	7.9%	74.9%		9.5%			
Activated carbon		474	9.6%	5.2%		3.1%			

* from 0 to 72.5 bar and curves overlap from 72.5 to 100 bar

Hysteresis loop % increases with temperature; the loop % is much higher for CO₂ compared to CH₄.

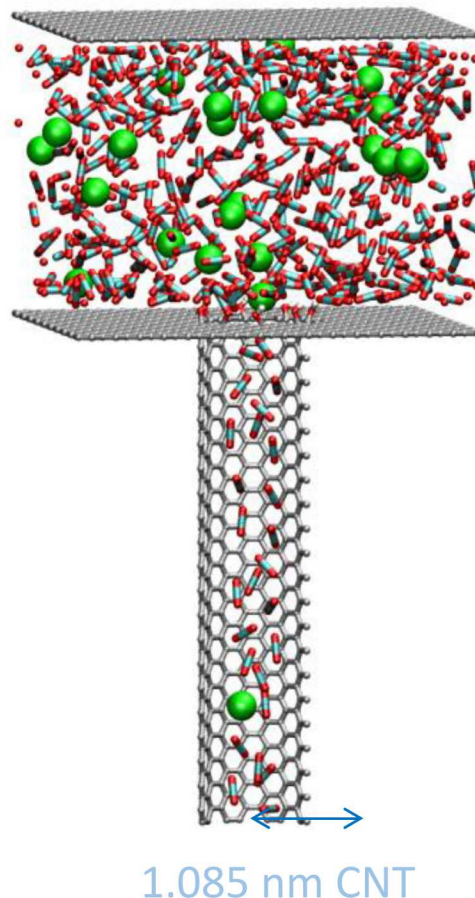
~~Current capillary condensation and pore neck snapping mechanism~~

More on CH₄-CO₂-H₂O in nanopores (Fuel 220, 1-7, 2018)



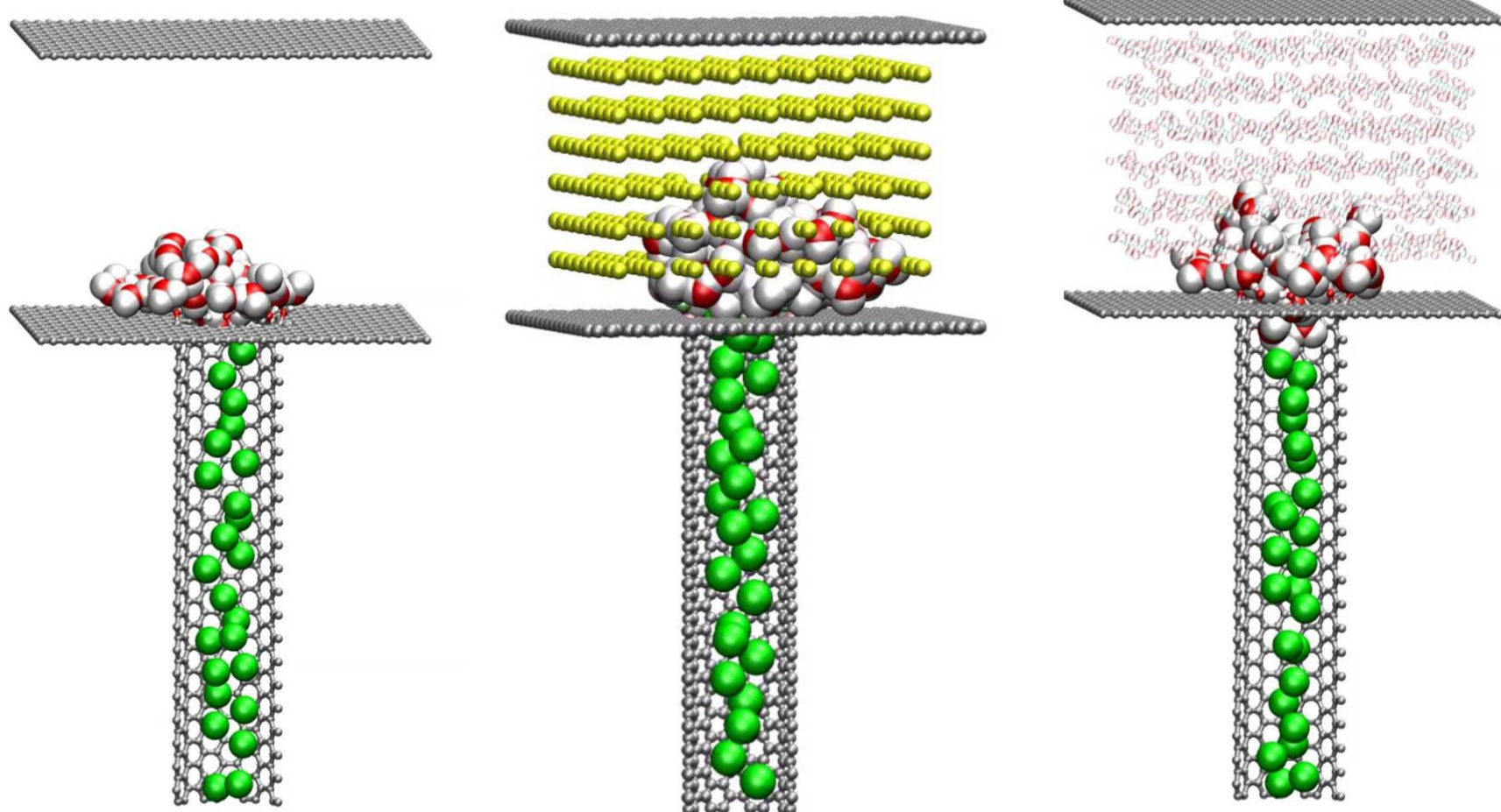
Pore is too small for the invasion of CO₂

Pore size effect



Pore is big enough for the invasion of CO₂

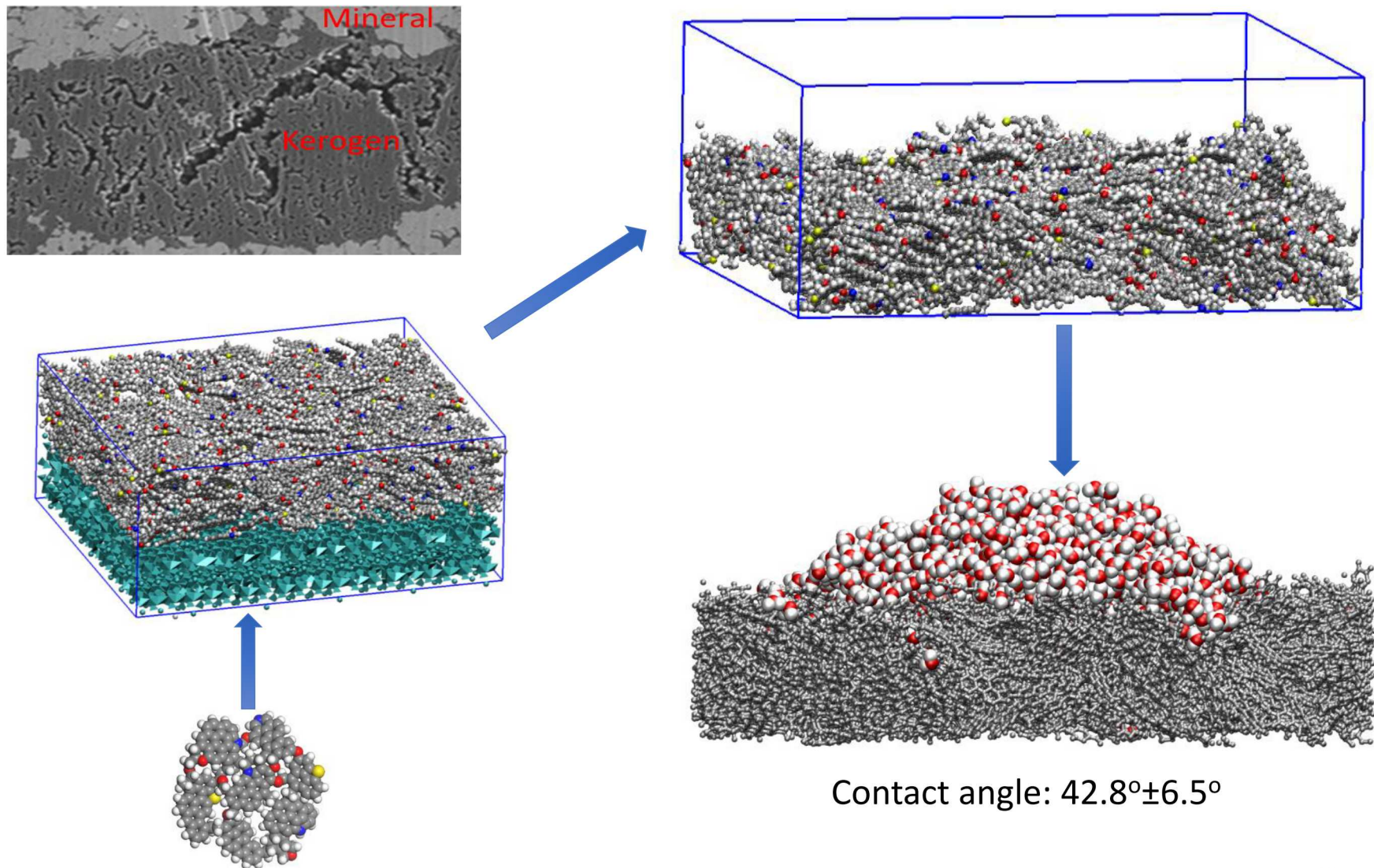
More on CH₄-CO₂-H₂O interaction in nanopores (cont.)



Water drop blocks the pore entrance.

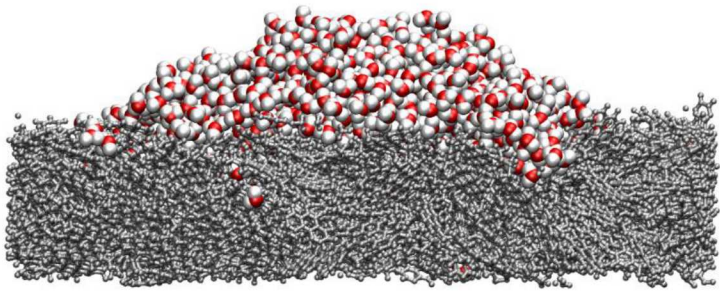
CO₂ invades through water and replaces CH₄ in the nanopore.

$\text{CH}_4\text{-CO}_2\text{-H}_2\text{O}$ interaction in a kerogen microfracture: Wettability (Nanoscale, 2018)

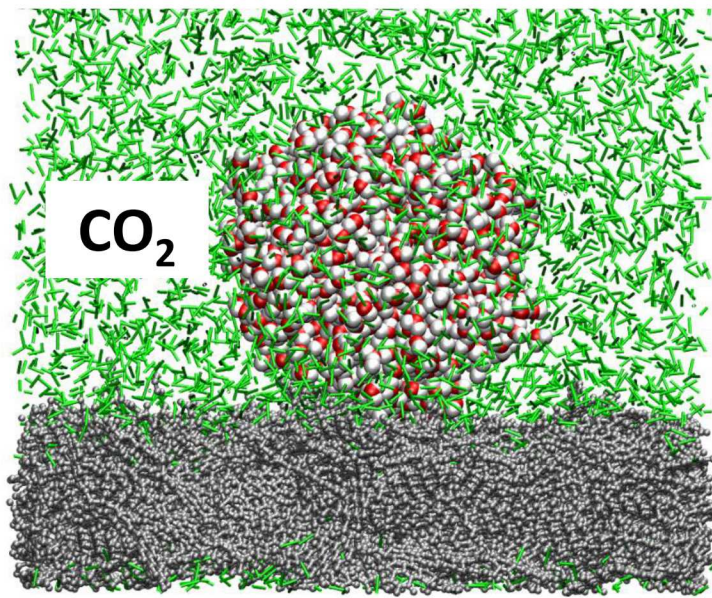
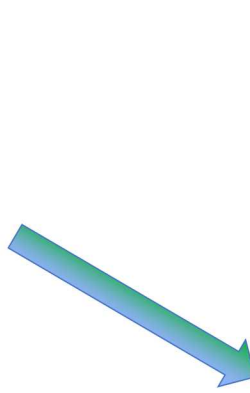
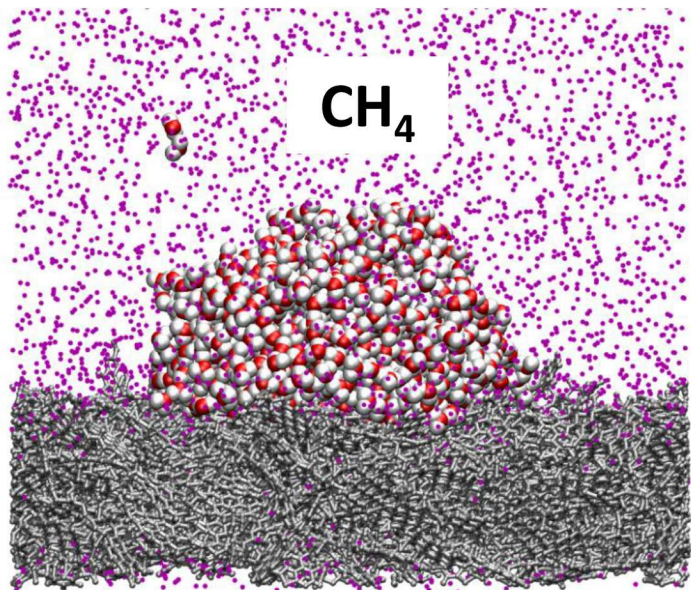


Wettability (cont.)

$42.8^\circ \pm 6.5^\circ$

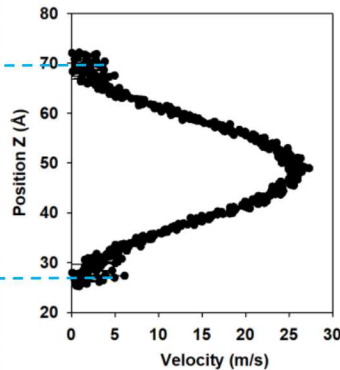
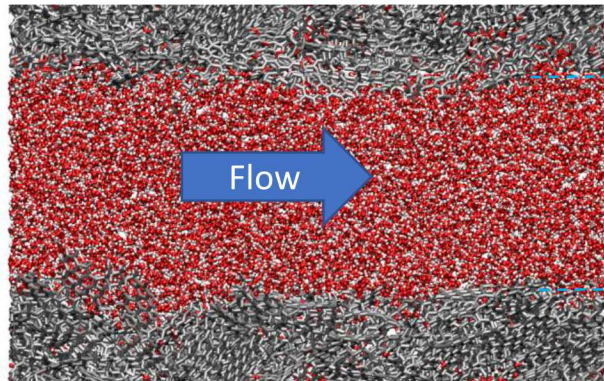


$79.18^\circ \pm 1.97^\circ$



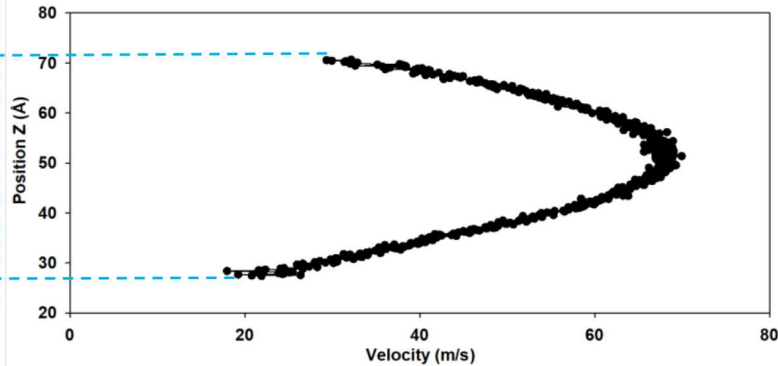
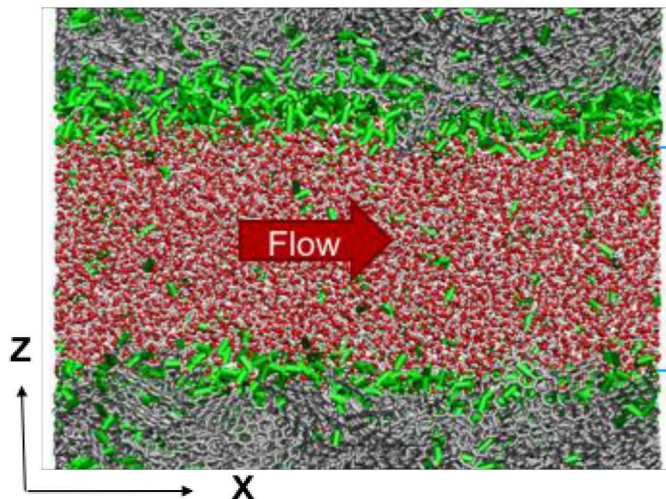
Hydrophilic to hydrophobic transition

$\text{CH}_4\text{-CO}_2\text{-H}_2\text{O}$ interaction in a kerogen microfracture: Fluid flow (Nanoscale, 2018)



$\frac{\text{Flow Rate (w CO}_2\text{)}}{\text{Flow Rate (w/o CO}_2\text{)}} \sim 4$

CO_2 thin layer \rightarrow Lubricant



Implications:

- Water release and removal
- Lubrication for hydrocarbon fluid flows?

Kerogen reaction with supercritical CO₂

Experiment: 0.13 gram immature kerogen reacted with supercritical CO₂ saturated brine (1M) at 90 °C and 2800 psi for 30 days

Observation: Some kerogen grains are reacted and coated by char, while others grains are not, indicating the heterogeneity (or selectivity) of the reaction.

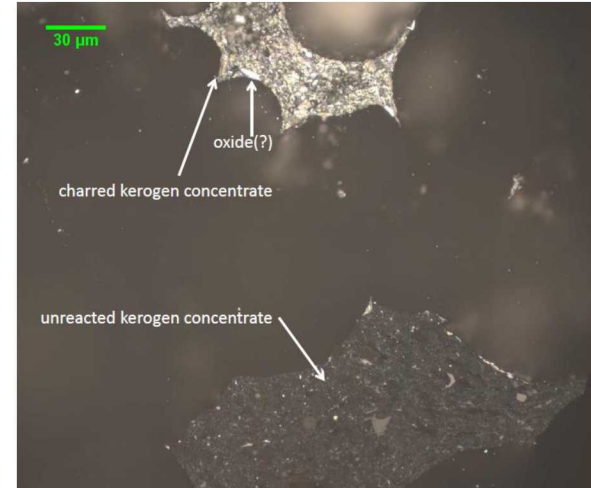
Original kerogen



Reacted kerogen



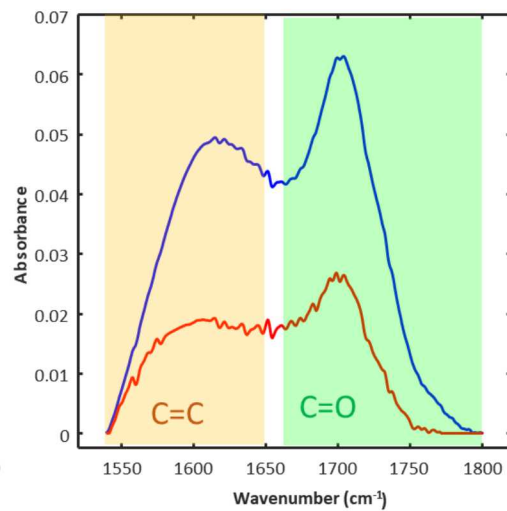
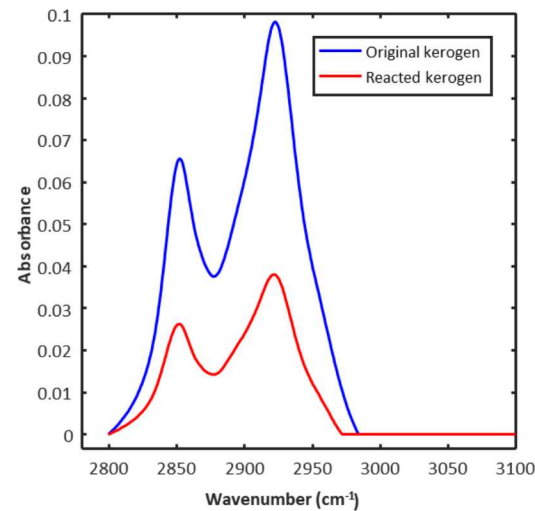
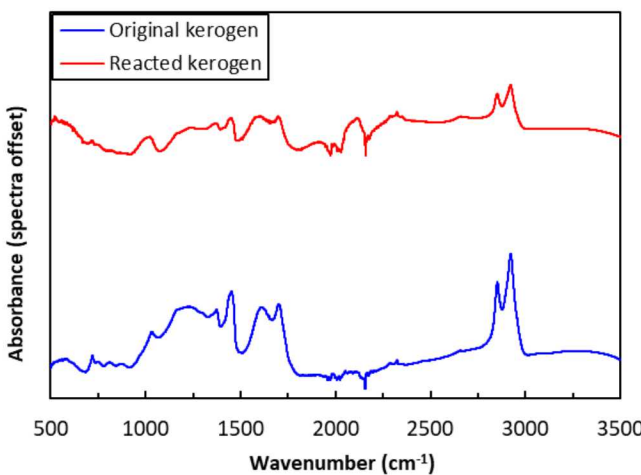
Reacted kerogen



Kerogen reaction with supercritical CO_2 : Change of functional groups

Observations:

- IR intensity of reacted kerogen decreases significantly, indicating the decrease in functional group abundance.
- At interval $2800 - 3100 \text{ cm}^{-1}$, the decrease is proportional, whereas at interval $1550 - 1800 \text{ cm}^{-1}$ aromatic $\text{C}=\text{C}$ decrease more than $\text{C}=\text{O}$ functional groups



Kerogen reaction with supercritical CO₂: Compositional changes

Observations:

- After reaction, C and H decrease and O increases.
- Pyrolysable carbon and residual carbon both decrease, presence of significant amount of inorganic carbon.

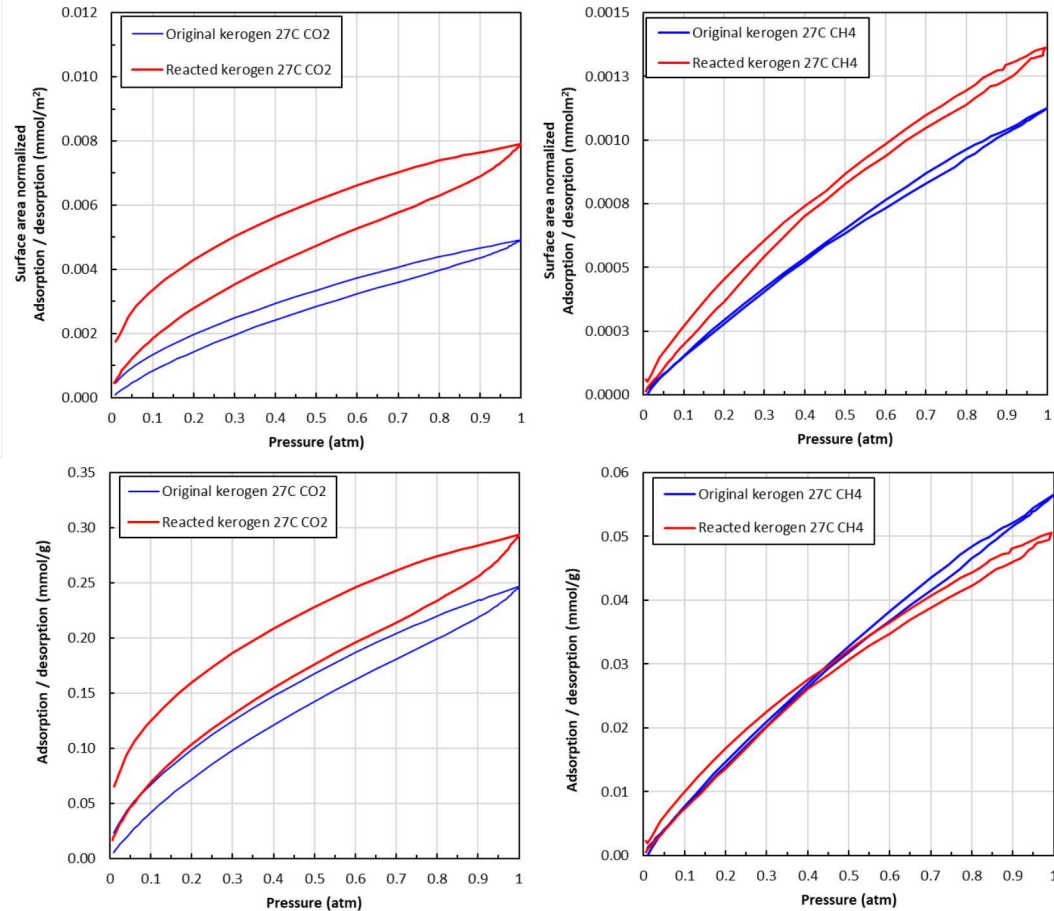
Implication: Chemical reaction with supercritical CO₂ as an alternative maturation?

	Carbon % w/w	Hydrogen % w/w	Nitrogen % w/w	Oxygen % w/w	Sulfur % w/w	Ash % w/w	C/H atom	C/O atom	C/N atom
original kerogen	73.91	7.59	2.67	8.40	2.73	3.0	0.81	0.73	32.3
reacted residual kerogen	62.68	4.54	1.64	12.36	1.49	24.10	1.15	0.42	44.6

	S1 mg HC/g	S2 mg HC/g	S3 mg CO ₂ /g	Tmax °C	Pyrolysable organic carbon % wt	Residual organic carbon % wt	TOC % wt	Hydrogen index mg HC/g TOC	Oxygen index mg CO ₂ /g TOC	Mineral inorganic carbon % wt
original kerogen	5.63	412.11	6.47	431	35.24	37.97	73.21	563	9	0.93
reacted residual kerogen	1.91	181.38	13.54	424	16.23	33.90	50.13	362	27	11.89

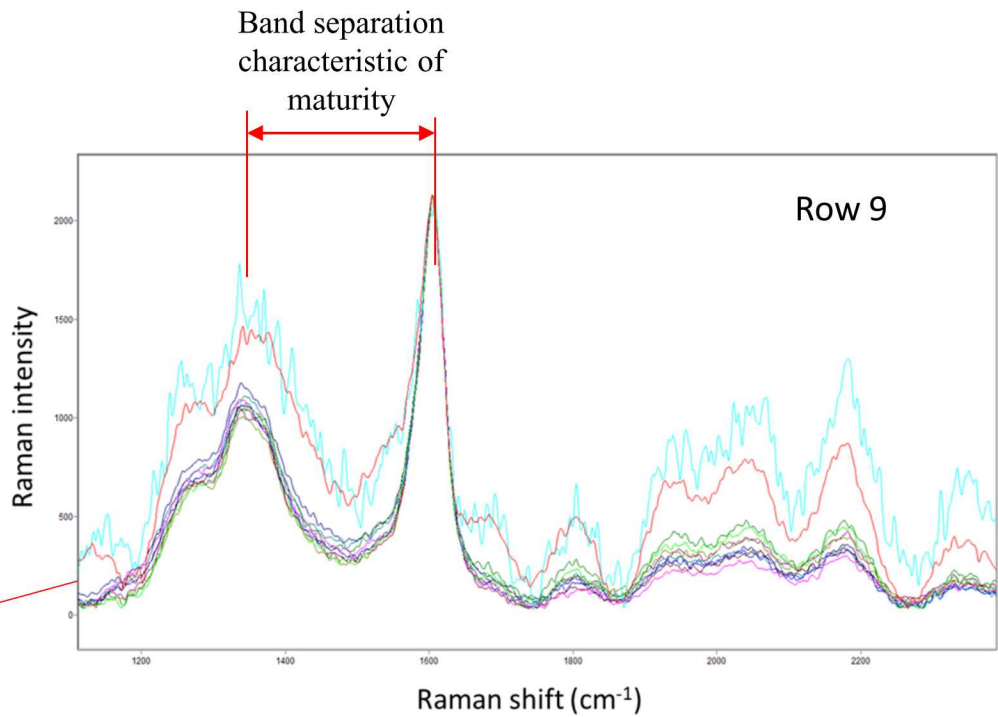
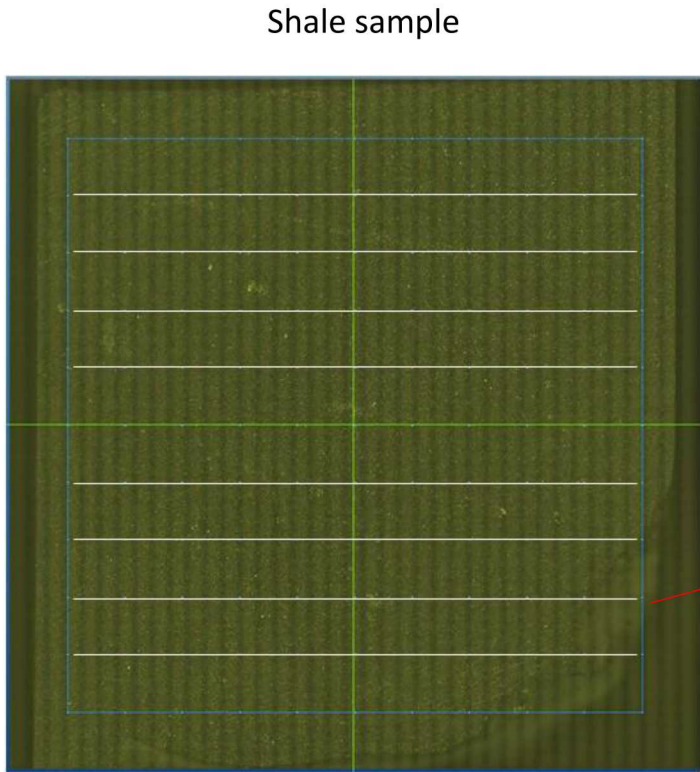
Kerogen reaction with supercritical CO_2 and its effect on gas adsorption

- After reaction, BET surface decreases from 50 to 37 m^2/g .
- Reacted residual kerogen adsorbs more CO_2 than original kerogen.
- Surface adsorption ability activation?
- CO_2 preferentially adsorbs to both reacted and unreacted kerogen.



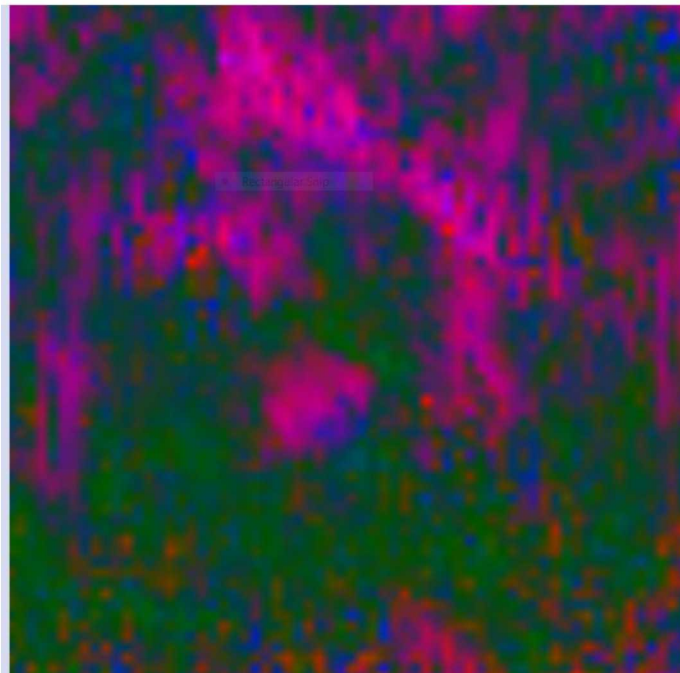
Physics-based, data-driven machine learning

Kerogen compositional variation by micro-Raman analysis



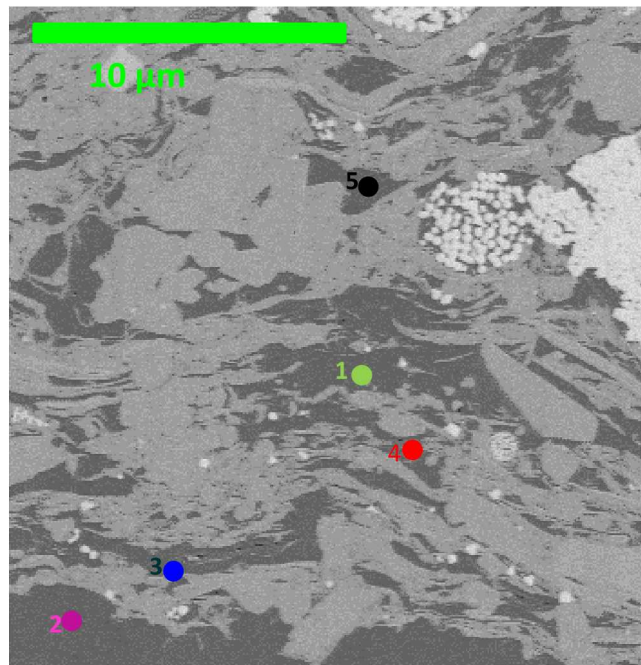
Micron- to Nano- scale kerogen compositional analyses

Kerogen compositional variation by micro-FTIR analysis



Green - organic
Pink - silicates

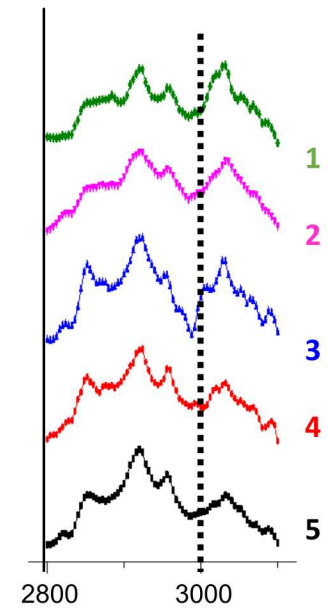
Kerogen compositional variation by NanoIR analysis



Collaborated with
Schlumberger –Doll Research

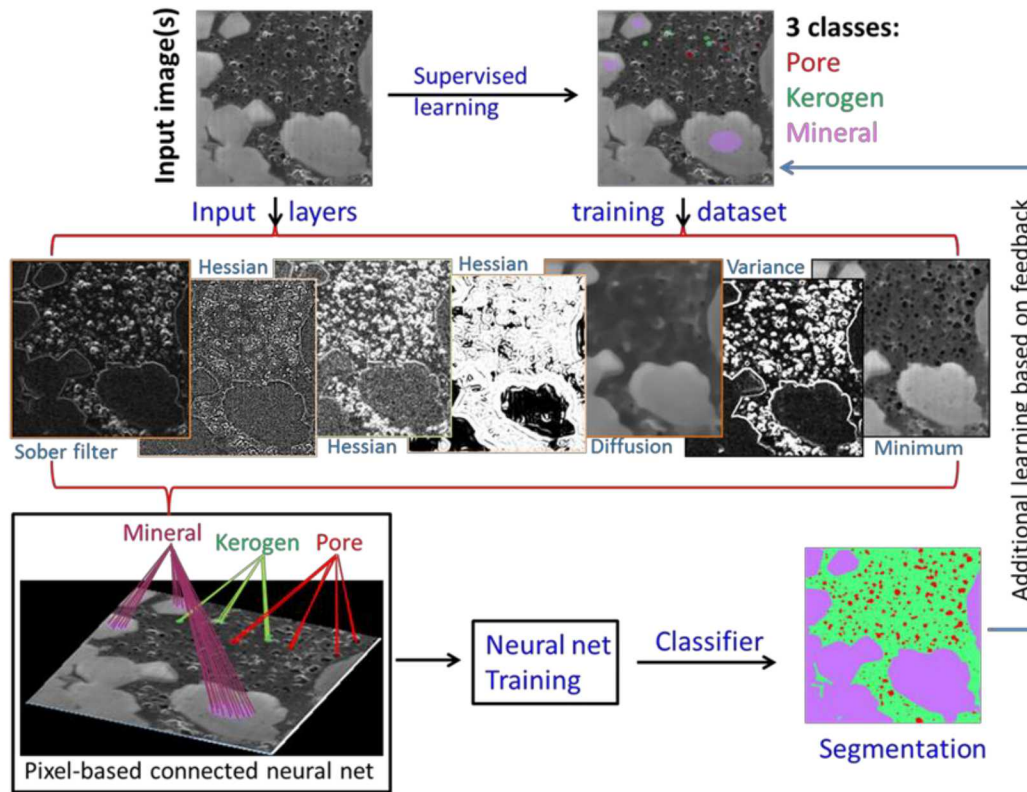
NanoIR spectra of different kerogen grains

- Strong aromatic absorption – mature kerogen
- Chemical composition variation between kerogen grains



Wavenumber (cm⁻¹)

Machine learning assisted microscopic image analysis



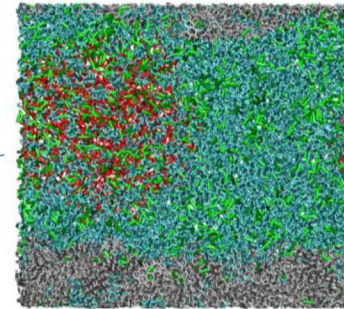
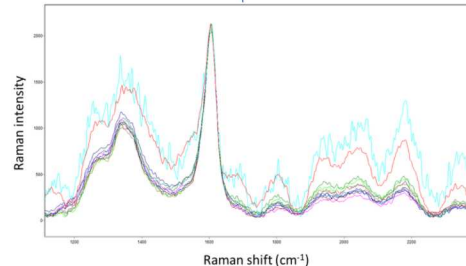
Goal:

- Unravel the functional relationship between kerogen maturity and local texture/composition.
- Construct 3-D nanopore networks.
- Develop continuum-scale constitutive relationships based on pore scale simulations.

Future work

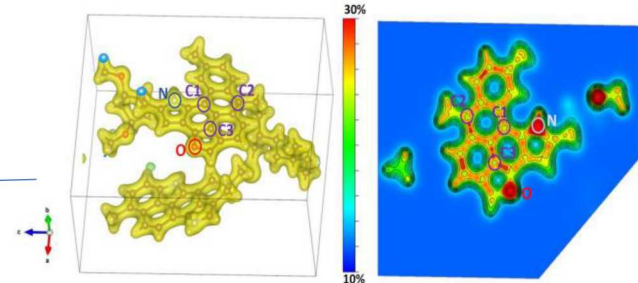
- Develop new kerogen models with better representation of functional groups (in progress).
- Extend the work to include other chemical components (e.g. LNG as a stimulating agent) (in progress).
- Understand $\text{CH}_4\text{-CO}_2\text{-H}_2\text{O}$ interactions in clay matrix (progress made, Sci. Rep., 2017)
- Use classical density functional theory (cDFT) to simulate and upscale molecular simulations (initiated).
- Develop EOS for $\text{CH}_4\text{-CO}_2\text{-H}_2\text{O}$ in nanoconfinement (to be initiated)
- Use DFT simulations to understand redox properties (e.g. electron transfer) of kerogen (initiated). (SNL-NETL-WVU)
- Understand isotope fractionation in nanoconfinement (initiated). (SNL-WVU)
- Use machine learning for image analysis and process model upscaling (initiated).

Data-driven ML



Red: Water
Green: CO_2
Cyan: Octane
Silver: Kerogen

Charge density isosurface of kerogen (type IIB) calculated using DFT



Using Real Time Gas Isotope to Model Gas Production Decline Curve

